Catalysis and Surface Organometallic Chemistry: A View from Theory and Simulations

Philippe Sautet* and Françoise Delbecq

Université de Lyon, Laboratoire de Chimie, Institut de Chimie de Lyon, École Normale Supérieure de Lyon and CNRS, 46, allée d'Italie, 69364 Lyon Cedex 07, France

Contents

1. Introduction

The development of new catalysts is a key objective for a cleaner and sustainable chemistry. Two important families of catalysts coexist nowadays. Metal complexes with ligands offer a flexible framework for molecular catalytic species, reaching high activity and selectivity for a large class of chemical reactions, finely tunable by changing the ligands. The structure of the catalytic complex itself can be studied by a variety of spectroscopic and crystallographic techniques, and although the exact nature of the active site in catalytic conditions is sometimes difficult to determine, a single molecular species is clearly responsible for the activity. The knowledge of reaction mechanisms and pathways is generally well advanced. The reaction is usually conducted in a homogeneous phase with the reactant and product, which leads to the well-known difficulty of separating the product from the catalyst. The necessity for a solvent is another constraint. On the other end of the spectra, heterogeneous catalysis uses a variety of solid surfaces (metals, oxides, sulfides) to accelerate a wide range of reactions. The large number of industrial processes using a solid catalyst is a clear demonstration of the efficiency of those catalysts. The surface of the solid presents a variety of sites, including defects such as steps with variable coordination for the active element. Moreover, the nature of the surface can change upon the

* To whom correspondence should be addressed. Fax: (+33) 472728860. E-mail: philippe.sautet@ens-lyon.fr.

Philippe Sautet has studied at "Ecole Polytechnique" in Paris and defended his doctorate in Theoretical Chemistry at Orsay University (Paris XI) in 1989. He then entered CNRS at the Institute of Research on Catalysis in Lyon, where he developed and led a group devoted to the applications of theoretical chemistry to heterogeneous catalysis. He is now director of the "Laboratory of Chemistry" at the Ecole Normale Supérieure of Lyon and at CNRS, and director of the "Institut de Chimie de Lyon". He has published over 190 scientific papers. He received the Descartes−Huygens prize in 1998, the silver medal of CNRS in 2007, and the Paul Pascal Prize of the French Academy of Science in 2008. His research interests are in the theory of the electronic structure at the solid−gas interface and the modeling of elementary steps of heterogeneous catalysis. Recent studies focus on the modeling of catalytic surfaces in realistic conditions and on the surface structure of alumina and its interaction with active sites, such as organometallic complexes. They also aim at exploring reaction pathways for molecules on these catalytic sites, with a special goal at understanding selectivity in heterogeneous catalysis. He collaborates with several experimental groups in the fields of surface chemistry and catalysis.

reaction conditions, and its structure is more difficult to characterize from microscopy and spectroscopy than it is for a molecular species. The determination of the active site is hence a challenge, and most probably several possible active sites compete on the solid surface. As a result, although the activity can be high and the products easily separable from the catalysts, heterogeneous catalysts generally suffer from a lack of selectivity. The fabrication of efficient enantioselective catalyst for fine chemical and pharmacological purposes is, for example, much less developed in heterogeneous catalysis than in the homogeneous field.

Surface organometallic chemistry attends to bridge the gap between these two fields. The organometallic chemist would say that it uses a solid surface as a ligand for the complex, hence attaching it to a particle. The solid-state chemist would say that the surface is modified by grafting a metal complex, hence creating a new catalytic species. The approach aims at creating a direct interaction between the metal and the

Figure 1. Example of cluster model for a surface organometallic system. A Zr complex is grafted on an alumina support, modeled by a cluster saturated by hydrogen atoms (Zr, blue; C, gray; Al, pink; O, red; H, white).

Françoise Delbecq graduated from the University of Lyon (France) in 1971 and obtained a Master degree in organic chemistry in 1972. At the same date she obtained a permanent position as a researcher at CNRS, Centre National de la Recherche Scientifique. She defended her Ph.D. in 1976 in the field of Organic Chemistry at the University of Lyon in the laboratory of Prof. Goré. She then moved to the laboratory of Prof. Salem at the University of Paris XI (Orsay) where she oriented her research toward Quantum Chemistry. She worked there on the mechanism of radical organic reactions. In 1985, she moved to the Institut de Recherches sur la Catalyse at Villeurbanne mainly devoted to the study of catalytic reactions. There she oriented her research toward the investigation of the mechanism of catalytic reactions by means of density functional theory (DFT) calculations with a particular focus on the selective and enanti-oselective reactions. Since 2003, she belongs to the Laboratory of Chemistry at Ecole Normale Supérieure de Lyon where she continues to work in the field of catalysis.

solid surface, and it is hence different from supported homogeneous catalysts where one of the ligands is attached to a solid surface at a position far from the metal. It has already led to several catalytic successes,[1−3] but opens a wide range of fundamental questions. What is the mechanism of the chemical reaction leading to the attachment of the complex on the surface? What are the possible interactions at its origin? Which species is formed? Is it unique, or do several forms coexist? What is the influence of the solid surface itself? How are the electronic properties of the metal modified? Are the functions of the complex kept, or new properties generated? Can unprecedented catalytic properties be obtained?

Those hybrid molecular-solid species, at the border between two different chemical fields, are difficult to characterize.[4,5] Computational methods[6] can hence be a very fruitful tool to better understand those fundamental questions. The purpose of this Article is to review the contributions of theoretical chemistry in this field of catalysis with surface organometallic species, in a broad definition, to summarize the insights that theory can bring to the above-listed questions. All types of surfaces and modes of interaction with the organometallic complex are considered, and structural, spectroscopic, and catalytic reactivity aspects are included.

2. A Brief Review of Methods and Tools

There are two main classes of models to simulate a metallic complex grafted on a solid support, also issued from the two fields that we discussed previously: molecular and solid-state chemistry. The molecular-based approach considers a fragment of the support surface and includes it simply as a ligand of the complex (Figure 1). In the past, the fragment of the surface was usually very small, which was a severe limitation for the representation of the support.
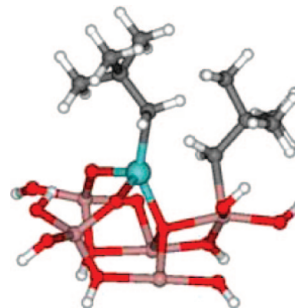
Nowadays, however, due to the growing computer power, large fragments can be considered. The termination of the fragment remains an important region, and, in the case of oxide materials, dangling bonds are often saturated by hydrogen or pseudohydrogen atoms. In some cases, the influence of the "missing" part of the solid can be described by a proper embedding technique, such as an array of point charges for an ionic solid, for example. The limitations of this approach are generally linked with the choice of a too small cluster and with the insufficient description of the environment of the chosen surface site.

This molecular approach (also called cluster model) for the support and grafted complex allows the use of the full machinery of molecular quantum chemistry. A compromise has to be achieved between the size of the model and the accuracy of the quantum mechanical description. Small models (10 atoms) can be tackled by highly accurate explicitly correlated techniques[7] (CASSCF, CI, ...), while more realistic models (from 10 to a few hundreds atoms) are generally considered with density functional theory (DFT),[8] which proposes an averaged and efficient way to treat the electron−electron interactions. Today, the various DFT approximations have become very popular, because they offer a good balance between accuracy and cost (hence, size of systems accessible). For large systems (large ligands remaining on the complex, for example), hybrid methods (QM/MM),[9] which combine a quantum chemical treatment for a core part, and a semiempirical approach for the surrounding can also be used.

The second class of models consists of describing the surface by a periodic slab, from a unit cell that is repeated in two directions[10] (Figure 2). In the direction perpendicular to the surface, the slab is composed of a finite number of atomic layers. A metal complex can be grafted on each of these unit cells.

When the grafted complex bares large ligands, the size of the unit cell must be big enough to avoid lateral interactions between neighboring complexes on the surface. Such periodic systems can be tackled with methods based on Bloch's theorem and coming from the solid-state community. These methods describe the electronic structure with the density functional theory,[11,12] with the Hartree−Fock method,[13] or recently for small systems with perturbation correlation techniques[14] (MP2). The surface is modeled as a two-dimensional extended system, with a finite number of layers in the perpendicular direction. This number of layers can, however, be varied until convergence of the desired property is obtained. Drawbacks arise from the fully ordered nature of the model surface, the possible lateral interactions between
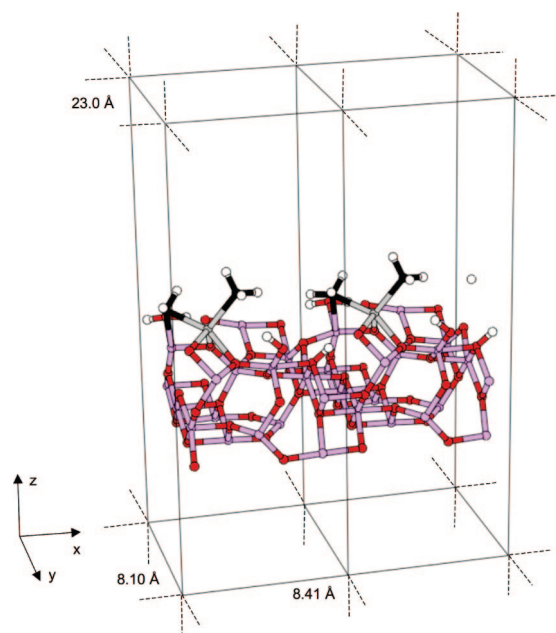
Figure 2. Example of a 2-D periodic slab model for a surface organometallic system, a Zr complex grafted on a periodic model of γ-alumina. Two boxes of the periodic system are shown.

the complex and its periodic images, and the more limited number of quantum methods available.

Both from the cluster and from the slab models, total energy calculations allow one to optimize the geometry of various structures for the grafted complexes, and to compare their stability. These structures can be compared to experimental results, for example to EXAFS data. Density functional theory generally gives molecular and solid structures that are in very good agreement with crystallographic results. The accuracy in the formation or adsorption energies is usually good but with a sizable error bar of $10-30$ kJ mol^{-1}. Indeed, if DFT formalism is exact in principle, one has to rely on approximate exchange-correlation functionals,[6-8] and this is the main source of error. Other approximations relate to numerical aspects, such as completeness of the basis set, number of k points, or use of effective core potential to describe atomic cores, but these points are usually well controlled in modern codes and lead to smaller errors in the formation energy. DFT is usually not very good at describing systems with weak interactions, such as dispersive van der Waals interactions. Explicitly correlated techniques are more accurate, but can only address small systems.

The comparison with experimental data can be enriched by the simulation of spectroscopic properties. Vibrational spectra can be simulated at various levels of approximations: harmonic approximation, anharmonic corrections, and calculations of the intensities. Methods to simulate NMR spectra have also been developed, both for molecular[15] and for solid-state[16] systems.

The exploration of catalytic mechanisms requires specific methods to follow reaction pathways from the reactants to the products, and to understand the influence of the grafted complex on this molecular reactivity. The "nudged elastic band" method[17] is widely used, together with ab initio molecular dynamics. The description of dynamic trajectories allows one to go beyond the static description of structure and reactivity and to incorporate fluxional behavior and temperature effects.[18]

Generally speaking, there has been a great evolution in the calculations, because of the development of new algo-

rithms and the growth of the computer power. Very large catalytic systems can now be simulated, in realistic conditions.

3. Mechanisms of Interaction between a Metallic Complex and a Solid Surface

Before considering the structure and properties of the surface organometallic complex, let us first describe the chemical mechanism leading to its formation, from a complex and specific reactive functions on the solid surface. Properties of the final grafted complex will be described in the following sections.

A large number of chemical mechanisms can be involved in the grafting of organometallic complex on a solid surface. We will only describe those that have been explored by a theoretical approach.

The simplest mechanism is obtained when one of the ligands of the complex possesses another chemical function, not implied for the interaction with the metal atom and free for a coordination with the surface. This process is, however, borderline of surface organometallic chemistry because the surface is not directly interacting with the metal atom. This is the case, for example, for Ru(4,4′-dicarboxylate-2,2′-bipyridine)(CO)$_2$I$_2$. The bipyridine part of the ligand is involved in the complexation with Ru, and hence the carboxylate function is free. It was shown to interact with Ti Lewis sites on anatase TiO$_2$(101).[19] Bidentate binding from the two carboxylate groups was found to be preferred despite the mismatch between the O−O distance between them (6.3 Å) and Ti−Ti distance on the support (Figure 3a). The flexibility of the ligand is here important for the bidentate coordination.

Another mechanism described by quantum chemical calculations is related to the nature of the Ti(IV) active sites obtained when grafting Cp$_2$TiCl$_2$ (Cp = cyclopentadienyl) complexes on mesoporous silica samples.[20] The grafting sites on the oxide support are the surface silanols. The calculations show that the first stable surface species result from a triple anchoring, ($\equiv$SiO)$_3$TiCp, consuming three surface silanols and replacing the two Cl and one Cp ligand around Ti. After calcination, ($\equiv$SiO)$_3$TiOH and ($\equiv$SiO)$_2$Ti(OH)$_2$ are formed, and they are more stable than the terminal oxo ($\equiv$SiO)$_2$Ti$=$O system (Figure 3b). These structures predicted after calcinations are in good agreement with EXAFS data, although EXAFS cannot easily distinguish between the mono- and dihydroxyl centers. Significant deviations between calculated and EXAFS structures are, however, observed for the cyclopentadienyl intermediate, especially in the Ti−C distance (2.4 Å in the calculation versus 2.0 Å from EXAFS). For the quantum calculations, the surface silanols are represented by minimal cluster models H$_3$SiOH, with some constraints in their positions. This is, however, a minimal approach to model the influence of the solid support. This is completed by a force field calculation for a large amorphous silica glass model of the silica substrate.

The global anchoring reaction is modeled, but the detailed elementary steps of the process are not described. The formation of the hydroxyl function from the ($\equiv$SiO)$_3$TiCp surface complex is considered as a hydrolysis reaction:

$$(\equiv SiO)_3TiCp + H_2O \rightarrow (\equiv SiO)_3TiOH + CpH$$

and subsequent hydration and hydrolysis of these surfaces models have also been modeled.
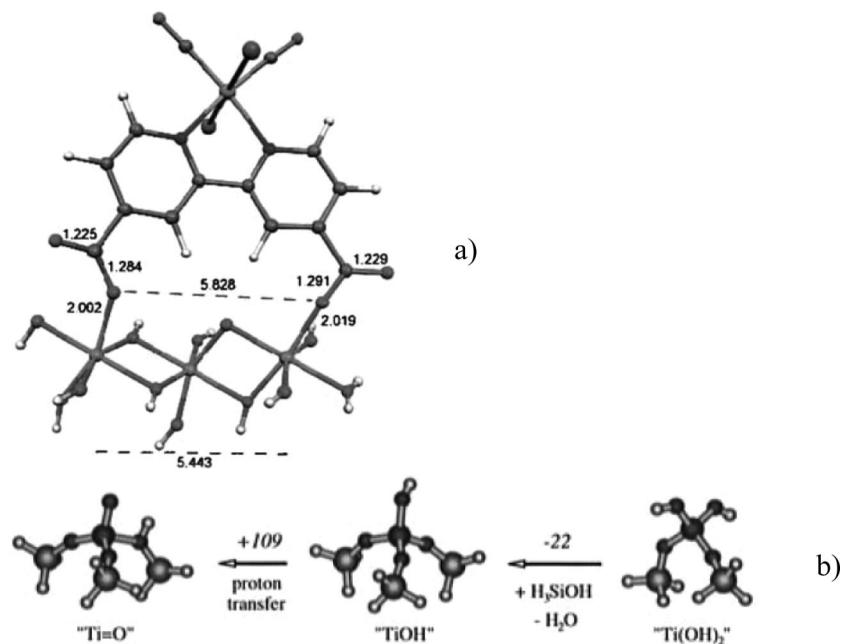
Figure 3. (a) Grafting of Ru(4,4′-dicarboxylate-2,2′-bipyridine)(CO)$_2$I$_2$ on TiO$_2$ anatase described with a cluster model. Reprinted with permission from ref 19. Copyright 2002 Elsevier. (b) Proposed structures and relative energies for the Ti(IV) active sites obtained after calcinations when grafting Cp$_2$TiCl$_2$ on silica. Surface silanols are represented by minimal H$_3$SiOH models. Reprinted with permission from ref 20. Copyright 1997 American Chemical Society.

Adsorption of dirhenium decacarbonyl Re$_2$(CO)$_{10}$ on γ-alumina follows from a different mechanism and implies different surface sites.[21] Oxygen atoms bridging two octahedral Al atoms, or bridging one octahedral and one tetrahedral Al, have been considered as grafting sites of the metal−carbonyl complexes, using cluster models for the γ-alumina surface. The grafting proceeds via a decarbonylation reaction, and the interaction energy of the unsaturated subcarbonyl complexes Re(CO)$_3$, Re(CO)$_4$, and Re$_2$(CO)$_9$ with the surface has been calculated. Binding energies range between 300 and 600 kJ mol^{-1}. The coordination of Al was found to have a considerable influence on the interaction energy, the mixed tetrahedral-octahedral site yielding a significantly stronger interaction. A decarbonylation scheme has been proposed (Figure 4). A first removal of a CO group on Re$_2$(CO)$_{10}$ enables one to attach Re$_2$(CO)$_9$ on the bridging oxygen. Heating then results in the breaking of the metal−metal bond and the initial formation of two grafted Re(CO)$_4$ centers. Further decarbonylation yields the formation of the stable Re(CO)$_3$/Al$_2$O$_3$. The reaction profile is globally significantly exothermic, from the strong bond formed by the unsaturated Re atom and the surface oxygen.

Another complex used to generate Re surface sites, active in olefin metathesis reaction, is CH$_3$ReO$_3$. Understanding the mechanism leading to the grafting of such complex on a silica, silica−alumina, or alumina surface is of key importance to determine the structure and chemical properties of the potential active sites. Two studies combining spectroscopic characterization and theory have appeared recently. The first one, combining NMR, IR, EXAFS, and DFT calculations, considers the grafting as a Lewis acid−base interaction, the organometallic species being kept intact.[22] The fully dehydrated silica−alumina support is described by a siloxane-capped aluminosilsesquioxane monosilanol cube, where Al has a tetrahedral coordination. In the most energetically favorable situation, one of the oxo ligands of CH$_3$ReO$_3$ interacts with the Al site. Comparison between EXAFS and DFT suggests that a five-coordinate Al is
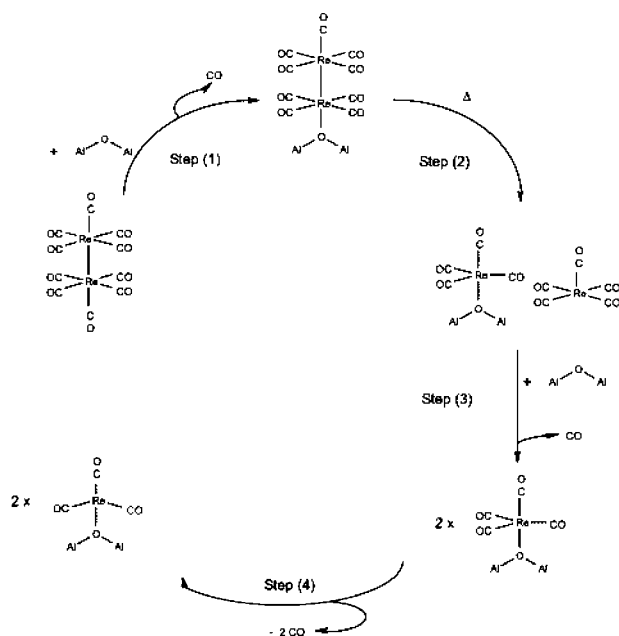
Figure 4. Proposed reaction mechanism for the adsorption and decarbonylation of Re$_2$(CO)$_{10}$ on a γ-alumina surface. Reprinted with permission from ref 21. Copyright 2001 Elsevier.

involved on the surface. An additional bond is created between an adjacent bridging oxygen atom (AlOSi) and the Re atom. Structural comparison between EXAFS and DFT leads to a very good agreement, with the Re=O bond involved in the grafting elongated by 0.1 Å. The authors hence conclude that the grafting creates a well-defined site with a two-point attachment, which is electronically different from the molecular precursor. The second study considers a partially dehydroxylated γ-alumina support with the same combination of techniques.[23] The γ-alumina support is modeled by a periodic slab.[24−26] The calculations show that indeed the main adduct results from the interaction between the oxo ligand and the Al Lewis acid sites (Figure 5a).
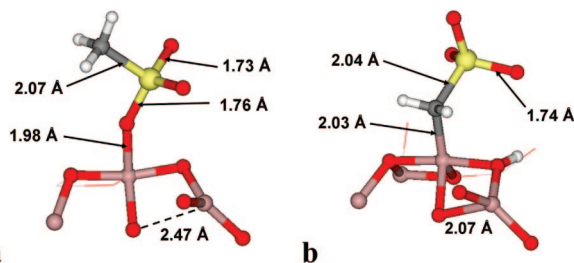
Figure 5. The two proposed grafting modes of CH_3ReO_3 on γ-alumina: (a) interaction of the oxygen lone pair with the surface Al lewis site; (b) dissociation of a C—H bond on a Al—O surface site. The second species is proposed to be the active site in olefin metathesis. Re, yellow; C, gray; Al, pink; O, red; H, white.

However, this majority species is not active for the olefin metathesis reaction. The active site is proposed to be a minority species resulting from the C—H activation of the methyl ligand of CH_3ReO_3 at reactive Al—O dehydroxylated sites of alumina (Figure 5b). This creates a surface hydroxyl group and a grafted surface Re methylene complex $AlCH_2ReO_3$, which is the initiating center for the carbene species propagating olefin metathesis.

From NMR, the surface density of these active Re methylene complexes was determined to be 0.15 per nm^2, as compared to 1.05 per nm^2 for the majority CH_3ReO_3 surface units. This completely agrees with the result of catalytic tests with labeled ethene, which shows that the catalyst contains about 14−15% of active sites, and that the methylene groups of those sites are involved in the formation of the propagating carbene species. Hence, the major surface species, which is seen by EXAFS spectroscopy, is not responsible for the catalytic event.

The grafting mechanism on γ-alumina was also detailed in the case of the chemisorptive interaction of two electron-poor complexes: $[Zr(CH_2{}^tBu)_4]$ and $[W(\equiv C^tBu)(CH_2{}^tBu)_3]$.[27] These are d^0 complexes, where the metal is at its highest oxidation state. This reduces the number of potential mechanisms for the grafting to alumina. The chemical active sites on the γ-alumina surface are the hydroxyl groups resulting from a partial hydration of the surface in usual operating conditions. The basic mechanism for the grafting process is a σ-bond metathesis scheme between Zr—C on the complex and O—H on the surface, to form the new Zr—O bond and a C—H bond with the evolution of an alkane molecule, consuming one of the alkyl ligands of the complex. This reaction can proceed several times for the same complex, leading to multipodal interactions between the complex and the surface.

The calculated energy pathway for the successive grafting steps of the model $Zr(CH_3)_4$ complex on γ-alumina is given in Figure 6. The initial grafting step proceeds as indicated with a σ-bond metathesis mechanism between one of the Zr—C bonds and the surface OH bond. The Zr—C and the OH bond are broken, while two new bonds are formed in a concerted manner: a Zr—O bond, covalently attaching the complex to the alumina surface, and a CH bond liberating a methane molecule in the gas phase. The transition state is a four-member ring with a triangular shape, the H atom being located along the O—C edge. The barrier for this elementary grafting step is small (37 kJ mol^{-1}), and the reaction is largely exothermic (200 kJ mol^{-1}). The system has then two possibilities to evolve further. A second Zr—C bond can interact with a neighboring OH group, forming a second covalent Zr—O bond, or, alternatively, one methyl ligand
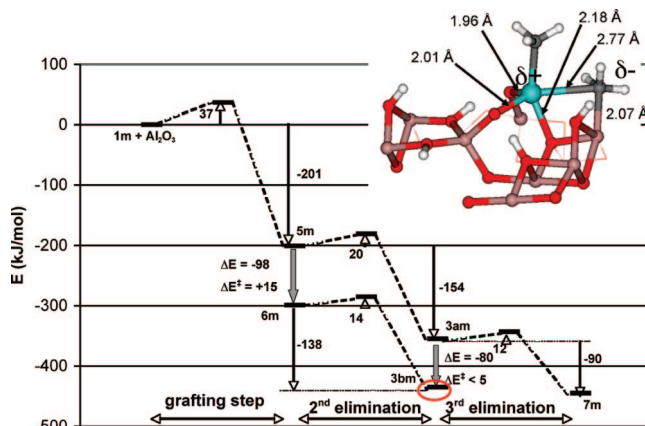
Figure 6. Calculated energy pathway for the successive grafting steps of the model $Zr(CH_3)_4$ complex on γ-alumina and structure of the proposed final surface complex (Zr, blue; C, gray; Al, pink; O, red; H, white).

Scheme 1. Two Possible Pathways for the Initial Grafting Step of the Model $W(CH_3)_3(\equiv CCH_3)$ Compound on γ-Alumina
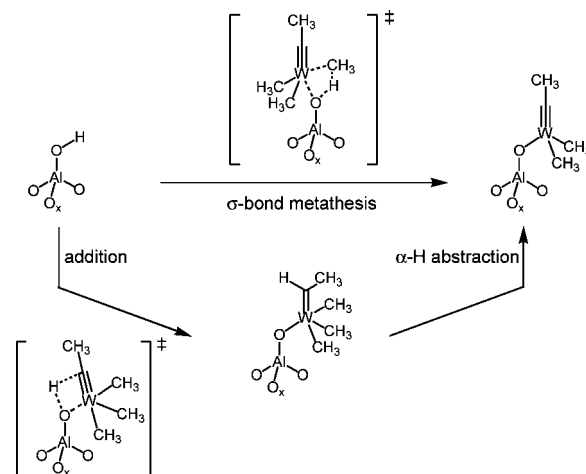
remaining on the Zr can shift to a neighboring Al Lewis acid center, hence creating an ion pair: $Zr^{\delta+}$, $Al(CH_3)^{\delta-}$. Both processes are easy and exothermic, and, in fact, they happen together successively in an indifferent order to yield the most probable grafted species, which is shown in Figure 6. The same process is involved when the real neopentyl ligands are considered. In that case, the neopentyl group is not bridged between the Zr and Al, but totally displaced on Al. Two covalent Zr—O—Al bonds are formed, liberating two neopentane molecules, in agreement with the mass balance analysis, and consuming surface OH bonds, as clearly seen in the evolution of IR spectra. A third neopentyl is shifted toward a surface Al, hence creating the ion pair, with a cationic Zr center bearing a single remaining alkyl ligand. The surface Zr complex is further stabilized by a dative bond from a surface aluminoxane Al—O—Al bridge toward the metal. A third elimination, although possible in principle, is excluded from a kinetic argument.

In the case of the W complex, for which alkyl and carbyne ligands are present, two reaction pathways are possible and have been compared (see Scheme 1). The first one goes through a σ-bond metathesis between W—CH_3 and O—H to form the O—W and H_3C—H bonds. The second one results from the addition of the hydroxyl group onto the carbyne to give a carbene, which undergoes an α-H-abstraction, thus releasing an alkane molecule in the gas phase and restoring

the W≡C bond. While the addition of an Al$_s$OH onto the carbyne requires one to go through a rather high activation barrier, that is, $\Delta_r E^{\ddagger} = 126$ kJ mol^{-1}, the direct electrophilic cleavage of the W−C bond by Al$_s$OH gives a much lower activation energy (81 kJ mol^{-1}), which shows that grafting probably occurs via the latter pathway, implying the alkyl ligand as it was the case for Zr. Elimination of a second alkyl ligand to form a bipodal complex involves a high barrier, especially if the complete ligands are taken into account (100 kJ mol^{-1}). It is hence proposed that the grafting process here stops at the monopodal complex. It can be underlined that activation barriers for the grafting are higher in the case of the W complex than for the Zr complex. This was explained by the rigidity in the complex due to the presence of the carbyne ligand, rending the deformation in the pentacoordinated structure of the transition state more difficult in the case of W. This is well in line with the slower grafting kinetics in the case of W.

A very natural approach to study the mechanism for grafting a complex on a surface is ab initio molecular dynamics, if this process involves energy barriers that are low enough to be passed after a rather short time for the trajectory (typically a few picoseconds). This approach was used to study the mechanism of deposition of Cu−hexafluoroacetylacetonato−trimethylvinylsilane on tantalum surfaces.[28] This relates to applications in microelectronics, but the fundamental aspects are very similar to surface organometallic chemistry. The dynamic simulations show that the Ta surfaces are very active and that the organic ligand undergoes spontaneous decomposition, which results in a very contaminated and disordered interface. Passivation of the surface by N$_2$, and formation of a surface nitride, strongly reduces their activity, and the ligand remains intact and can be liberated to the gas phase, with the formation of a clean interface with Cu.

4. Nature and Structure of the Surface Organometallic Species. Identification of the Surface Catalytic Active Site

A large number of theoretical studies are devoted to the determination of the structure and electronic properties of grafted organometallic complexes. Such approaches are generally conducted in parallel with experimental characterizations such as EXAFS, NMR, or vibrational spectroscopy, which would be very difficult to interpret alone. There are very good illustrations of the potential synergy between such experimental data and simulations, toward a better understanding of these complex surface structures.

Indeed, it is generally not easy to determine which complex-surface structure represents the observed surface complex as indicated in the methods section. Three types of models are used for these calculations.

4.1. Clusters as Surface Models

Initially, the oxide surface, in many cases silica, was modeled by a small cluster with one, two, or three Si atoms (or equivalent). These small models have been very helpful in understanding the main characteristics of the bonding between the surface site and the metal complex. They bear, however, a number of limitations, inherent to the small size of the model and to the incomplete description of the environment of the grafting site. A large class of systems has been described with such a cluster approach.
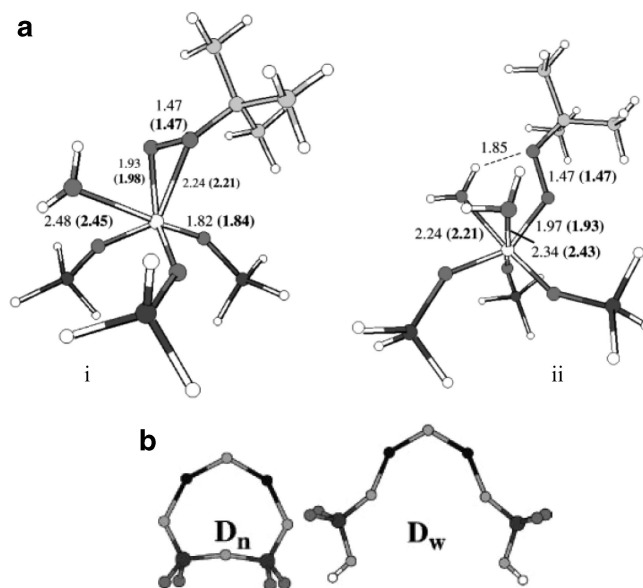
Figure 7. (a) Proposed Ti-peroxo species. All distances are shown in angstroms, and experimental values are given in parentheses (i, η^2; ii, η^1). Reprinted with permission from ref 29. Copyright 2002 PCCP Owner Societies. (b) Structure of dinuclear Cr(II) models on silica, in a constraint (*Dn*) or in an open (*Dw*) geometry. The elements are coded on a gray scale according to increasing atom number, H (white) < O < F < Si < Cr (dark gray). Reprinted with permission from ref 32. Copyright 2002 Elsevier.

A combined DFT-EXAFS study has been proposed in that spirit to investigate the structure and coordination of the oxygen donor for the oxidation catalysts formed by Ti in MCM-41 exposed to *tert*-butyl hydroperoxide.[29] Several Ti(η^2-peroxo) and Ti(η^1-peroxo) species have been considered, both with the model hydrogen peroxide and with the completely substituted oxygen donor. In contrast with previous estimates,[30] the calculations show that Ti(η^1-OO^{t}Bu) is significantly more stable than the η^2 structure.

A 6-coordinate Ti(η^1-OOR) species (R = H or R = ^{t}Bu) is then proposed for the peroxide/titanosilicate complex. EXAFS confirms the 6-coordinate species of Figure 7a but is unable to distinguish between η^1 and η^2, both structures giving equally good fits. Other species such as η^2-O$_2$, η^2-OO$^-$, and η^1-OO$^-$ are ruled out. A previously unidentified complex Ti(η^1-O$_2$H$_2$) is found to be stable with respect to reactant from the calculations, but does not fit well the experimental data.

Such Ti-based oxidation catalysts can be modified by ligands with Lewis base properties, to change the Lewis acidity on the Ti center and to control the activity and selectivity of the catalyst.[31] Various O−O, O−N, and N−N bidentate ligands were compared. The Lewis acidity of the surface complex was tested by the coordination of a NH$_3$ molecule. The energy level of the LUMO of the surface complex, an indicator of the Lewis acidity, was shown to give a very good correlation with the activity and the selectivity of the catalyst for cyclohexene epoxidation (the lower is the LUMO energy, the higher are the activity and selectivity). Theory hence appears here as a very useful tool to design new active and selective catalysts, within this class of compounds and structures.

In the context of Phillips catalysis for the polymerization of ethene, mononuclear Cr(II) and Cr(III) sites, as well as dinuclear Cr(II) sites, have been studied on silica models (cf., Figure 7b) using density functional theory.[32] For a
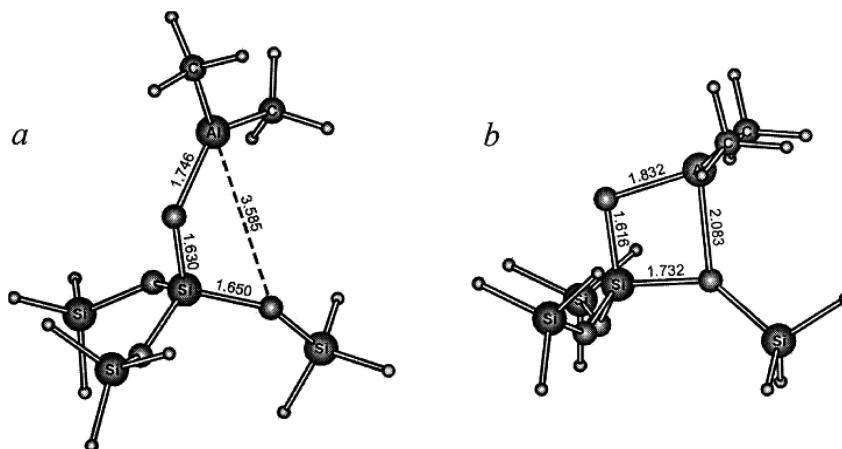
Figure 8. Two structures for aluminum trimethyl grafted on an OH group of silica. One methane molecule is evolved in the gas phase. Optimized structures are obtained from MP2 calculations. Reprinted with permission from ref 39. Copyright 2000 Elsevier.

detailed characterization, calculated harmonic frequencies and infrared intensities for CO exposed catalysts are compared to experimental spectra. The mononuclear Cr(II) site, with a pseudotetrahedral structure, adsorbs two molecules of CO, and, together with monocarbonyl species, they explain the triplet band found in room-temperature spectra. The evolution of this spectra with increasing CO pressure is explained first by dicarbonyl and tricarbonyl species at dinuclear divalent chromium sites, and then by the formation of tricarbonyl complexes at mononuclear Cr(III) sites. An important consequence of this reassignment is that dichromium species exist in significant amount on the catalyst.

Ni(II) sites on silica have been tackled with a similar approach.[33] One type of monocarbonyl species, 3-fold coordinated on the silica, is formed on Ni(II) ions. Only the model cluster bearing a −1 charge allows reproducing the Ni−O distances obtained from EXAFS and yields a CO frequency in agreement with experimental data. It is also shown that the charge of the cluster strongly influences the CO vibration, while the size of the cluster has a much smaller effect. This suggests a rather local nature of the metal−substrate interaction.

A similar approach was carried out for amide−copper−silica systems,[34] as models for C−Cl bond metathesis catalysts, and for silica-supported Mo−allyl,[35,36] or uranyl complexes.[37] In the latter study, two types of bridged structure for uranyl silicates have been proposed, which are consistent with the EXAFS data. A series of metal aquo-complexes has also been studied, interacting with disiloxane sites (metal ions = Mg, Ca, Sr, Ba, Zn, Cd, and Hg).[38] One water molecule in the aquo-complex is simply replaced by an oxygen atom of a Si−O−Si bridge on the silica surface. The formation energy of the metal aquo-ion/disiloxane system and the inverse of the metal−oxygen bond length in the metal aquo-ions are shown to be pertinent descriptors of the stability constant for surface complexation.

The coordination of methyl aluminum, zinc, and boron derivatives on silica was also studied with small clusters in the context of chemical vapor deposition for electronic materials.[39] Indeed, metal alkyls are promising precursors for gas-phase epitaxy, thin film growth, and novel surface design. The metal alkyl molecule $M-(CH_3)_n$ reacts with the surface OH group, with a σ-bond metathesis type reaction (cf., section 3), to form the grafted metaloxy derivative $Si-O-M-(CH_3)_{n-1}$, one methane molecule being liberated in the gas phase. A specificity of aluminum trialkyl is to

yield a cyclic structure arising from an additional Lewis acid−base interaction between Al and an oxygen neighbor of the Si grafting site (Figure 8). Calculation of the free energy shows that the cyclic structure is slightly less stable than the structure without this extra Lewis acid−Lewis base interaction (by 0−4 kJ mol^{-1} depending on the method).

Not only oxide supports can be addressed, and, for example, Ziegler−Natta polymerization catalysts can be modeled by the interaction between a $TiCl_4$ unit and a $MgCl_2$ support, here described as small clusters (with 1 or 2 Mg ions).[40] The structure of the supported complex resembles the chain-like structure of β-$TiCl_3$, with a vacant site on the octahedral environment of Ti that allows the further coordination of the alkene, the first step of the polymerization process (see also section 5.3).

The interaction between transition metal carbonyl complexes and oxide supports has also been the subject of numerous studies, using such a cluster approach. The decomposition of Re carbonyls on MgO powder results in $Re(CO)_3{}^{n+}$ fragments in interaction with the oxide, which have been characterized by DFT calculations, in relation with EXAFS and IR spectra.[41] Both dehydroxylated and hydroxylated MgO surface cluster models were considered.

The surface acts as a polydentate ligand, creating new adsorbate−surface (Re−O) bonds that are as strong as metal−ligand bonds in usual transition metal complexes. Hydroxylation of the oxide support can strongly reduce the adhesion between the organometallic fragment and the surface. The calculated structural and vibrational parameters are in good agreement with experimental data, including the strong red shift for $\nu(C-O)$ frequency observed on hydroxylated versus dehydroxylated sites. This approach was further extended to other examples such as cationic Rh dicarbonyl complex embedded in the cavities of dealuminated Y zeolite.[42,43] In this case, EXAFS cannot directly determine the location of the complex in the cavities, because three different models (with different number of O atoms of the zeolite interacting with the Rh) are compatible with the data. This indetermination has been resolved by the DFT calculations and their correlation with the EXAFS and IR results. The proposed planar ML4 structure, shown in Figure 9, gives very good agreement between calculations and experiments for the bond distances and the CO frequency shifts. This study clearly illustrates the synergy between theory and spectroscopy to determine the structure of a metal complex anchored to a structurally well-defined oxide support. Using
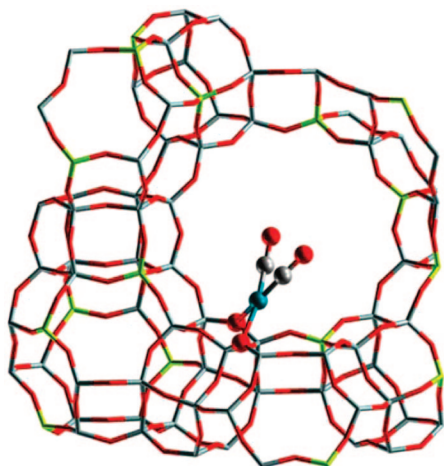
Figure 9. Proposed structure for the cationic Rh dicarbonyl complex in the cavity of dealuminated Y zeolite from a combination of EXAFS and DFT calculations. Rh, blue sphere; C, gray sphere; O, red sphere and stick; Si, blue stick; Al, green stick. Reprinted with permission from ref 42. Copyright 2004 Elsevier.
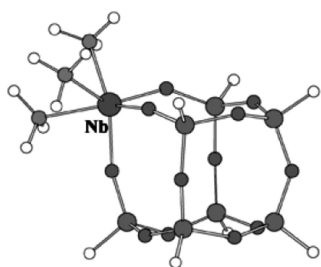
Figure 10. Proposed structure of niobium−silsesquioxane complexes coordinating three methyl ligands (anion). Reprinted with permission from ref 47. Copyright 2002 Elsevier.

the same computational approach, the structure of Rh(I) monocarbonyl species in zeolite was determined and their IR frequency assigned.[44] It was shown that the weak band at 2093 cm^{-1} is not associated with RhCO$^+$, as assumed before, but corresponds to species with additional hydrogen or dihydride ligands, such as Rh(H$_2$)CO$^+$ or RhH$_2$CO$^+$.

To complete this paragraph on carbonyl complex, we should also mention a study of Co carbonyls in interaction with silica, where different types of bonding are compared: (CO)$_x$Co−Si, (CO)$_x$Co−O−Si, and (CO)$_{x-1}$Co−CO−Si. Bonding via the carbonyl ligand was found to be the weakest interaction, while the strongest one is obtained by bonding with surface oxygen.[45]

4.2. Molecular Models as Supports

In recent calculations, larger clusters tend to be used. An elegant bridge between simulation model and reality is to use molecular models of oxide particles, such as silsesquioxane or polyoxometalates. The silsesquioxane ligand (formula R$_7$Si$_8$O$_{12}$O) has a cubic shape with the 8 Si atoms in the corners and 12 O atoms in the middle of the edges. The electronic properties of the model ligand L = H$_7$Si$_8$O$_{12}$O were characterized on a L$_2$TiH$_2$ complex by DFT calculations.[46] It was found to be less electron donating than the Ph$_3$SiO ligand, in good agreement with the lower deprotonation energy and pK_a value of H$_7$Si$_8$O$_{12}$(OH) as compared to Ph$_3$SiOH. The transition metal atom can also be incorporated in the cube framework. This is the case for niobium−silsesquioxane complexes (see Figure 10), which have been studied as models for silica-supported transition-metal catalysts and compared to niobium coordination complexes.[47]

The structure around Nb can be described as trigonal antiprismatic. The Nb(CH$_3$)$_3$ fragment is easily accommodated by the silsesquioxane, due to the flexible nature of the Si−O−Si framework (especially the Nb−O−Si angle). The electronic structure is simple, with a closed-shell singlet ground state.

Polyoxometalates are also interesting molecular supports to graft transition metal complexes. Ru^{II} and Os^{II} derivatives have been incorporated in the monolacunary Keggin anion [α-PW$_{11}$O$_{39}$]$^{7-}$, and they show a bidentate coordination on two nonequivalent oxygen atoms of the lacuna. The obtained complexes have been studied by DFT calculations.[48]

These calculations show that the observed nonsymmetrical coordination mode is not governed by charge control but by orbital interactions. The shape of the HOMO of the lacunary anion in the geometry from X-ray structures explains the bidentate and regiospecific linkage. The three possible regioisomers resulting from the bidentate grafting of the complex have been studied (Figure 11). The nonsymmetrical one implying two nonequivalent O atoms (noted R(O$_1$O$_4$)) is indeed the most stable one, but the two others regioisomers are only slightly less stable.

4.3. Periodic Systems as Models of Supports

A third class of models, which is getting more and more popular, is to describe the oxide support with a periodic slab, studied with periodic calculations. In these cases, the extended nature of the support is well described. The periodic

R(O$_1$O$_4$)	R(O$_1$O$_2$)	R(O$_3$O$_4$)
0.0 (0.0)	1.2 (2.8)	5.8 (2.8)

Figure 11. Optimized structures, labeling, and energies of the three regioisomers of [α-PW$_{11}$O$_{39}${Ru(η^6-C$_6$H$_6$)(H$_2$O)}]$^{5-}$. Energies (in kcal mol^{-1}) are given relative to the most stable isomer (values in parentheses include the effect of the water solvent treated as a continuum). For reasons of clarity, the hydrogen atoms on the benzene ligands are not represented. Reprinted with permission from ref 48. Copyright 2006 American Chemical Society.

Figure 12. Optimized structures for $[(\equiv SiO)Re(\equiv C^tBu)$-$(=CH^tBu)(CH_2{}^tBu)]$ using cristobalite as a surface model. Re, blue; C, gray; Al, yellow; O, red; H, small white. Reprinted with permission from ref 49. Copyright 2006 The Royal Society of Chemistry (RSC) for the Centre National de la Recherche Scientifique (CNRS) and the RSC.

and hence perfect "crystalline" nature of the model is, however, a limitation, because in most cases the support is a high surface area powder.

The silica-supported olefin metathesis catalyst $[(\equiv SiO)Re(\equiv CR)(=CHR)(CH_2R)]$ (R = Me and R = ^tBu) has been modeled in such a way.[49] This case is especially interesting because the supported system is highly active for olefin metathesis, while molecular analogues $[(X_3SiO)$-$Re(\equiv CR)(=CHR)(CH_2R)]$ (X_3SiO is triphenylsiloxy or polymeric silsesquioxane) are inactive. The cristobalite and edingtonite ideal surfaces are used in the calculations. The calculated structure agrees with EXAFS data and also yields very good comparisons for the alkylidene ligand J_{C-H} coupling constants and ν_{C-H} stretching frequency. This alkylidene fragment shows two conformations (syn and anti, see Figure 12), and the associated isomers are close in energy, the syn with the R ligand pointing away from the surface being always more stable. The striking result, however, is that the geometry and electronic structure of the Re species are essentially the same when grafted on the silica surface, or when attached to the molecular analogues. The calculations suggest that the siloxy group of the first coordination sphere of Re determines the metal properties. The silica surface hence appears just as a bulky chelating ligand, electronically equivalent to other simpler siloxy groups. Therefore, the specific catalytic reactivity of the supported organometallic complex is not related in this case to an electronic effect induced by the support. The more likely influence of the solid support is to separate the highly reactive intermediates and to prevent their deactivation via dimerization, which is difficult to avoid in liquid phase. A similar approach has been used in the case of $[(\equiv SiO)W(=NAr)(=CH^tBu)(CH_2{}^tBu)]$.[50]

Beside silica, the alumina support has also been described by using periodic models. We have already mentioned in section 3 the study of the grafting mechanisms of Zr and W complexes on γ-alumina.[27] In the case of the Zr tetra-neopentyl complex, a cationic bipodal structure was proposed (see Figure 6) with one of the two remaining alkyl ligands shifted toward an Al atom on the support. This surface species has been further validated from the simulation of the ^{13}C NMR spectra, and it has been shown that the neopentyl ligand interacts with a tricoordinated Al (Al$_{III}$, defect). A similar system has been recently considered by Marks et al.[51] with $Cp_2Zr(CH_3)_2$ grafted on fully dehydroxy-
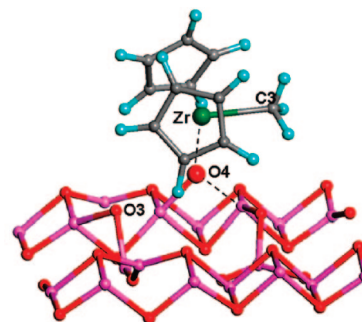
Figure 13. Most stable adsorption mode of cationic $Cp_2Zr(CH_3)^+$ on dehydrated alumina. Zr, green; C, gray; H, blue; Al, pink; O, red. Adapted and reprinted with permission from ref 51. Copyright 2008 American Chemical Society.
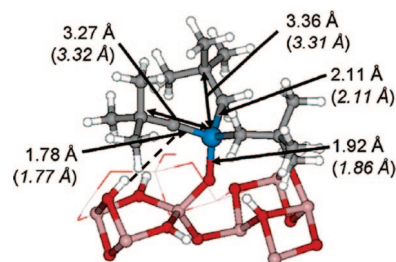
Figure 14. Optimized structure of $[(\equiv Al_sO)W(\equiv C^tBu)(CH_2{}^tBu)_2]$. The distances from the EXAFS analysis are indicated in parentheses. W, blue; C, gray; Al, pink; O, red; H, white. Reprinted with permission from ref 27. Copyright 2006 American Chemical Society.

lated γ-alumina (110) (Figure 13). A periodic approach is used, the electronic wave function being expanded in atom-centered basis functions. Because OH groups are not present in that case, the above-described elimination of CH_4 from a CH_3 ligand cannot happen, and grafting proceeds by the formation of an ion pair $(Cp_2Zr(CH_3)^+CH_3{}^-)$. The cation interacts with the surface O atoms (dioxo-bridged or oxo-bridged structure at both the μ_2-O and the μ_3-O sites), while $CH_3{}^-$ interacts with a 3-fold surface Al, as evidenced by NMR.

In the case of the W complex $[W(\equiv C^tBu)(CH_2{}^tBu)_3]$, the structure of the grafted complex on a surface hydroxyl group of γ-alumina, involving elimination of one neopentyl ligand (see section 3), has been validated by a combination of DFT calculations, EXAFS spectroscopy, and IR spectroscopy.[27,52] The optimized structure of the grafted complex is shown in Figure 14, together with the distances obtained from the EXAFS analysis. The agreement is very good.

A second way to evaluate this model is to consider how the stretching frequencies of the remaining surface OH groups on alumina are affected by the grafting of the complex.[27] Experimentally, after the grafting process, some of the OH vibrations are shifted and a broad signal at 3650 cm^{-1} appears. This was interpreted as resulting from an interaction between the surface OH groups and ligands remaining on the complex. Several azimuthal orientations of the complex can occur, leading to different interactions. In the structure of Figure 14, one surface OH weakly interacts with the π system of the carbyne ligand (dashed line), and its stretching frequency is decreased from 3700 to 3630 cm^{-1}. Other conformers give a smaller decrease of the frequency. There is hence a clear indication that complex$-$surface interaction affects the properties of the remaining surface OH. This effect is intrinsic to cases where a large number

of ligands remain on the complex and was not seen, for example, in the previous case of zirconium.

Finally, this structure allows one to reproduce the six major peaks in the ^{13}C NMR spectrum of the W complex. Again, the interaction between surface and ligands is important, now affecting the NMR chemical shifts of the C atoms on the ligands. Two conformers exist, one showing an interaction of a vicinal OH group with the carbyne and the other with its neopentyl ligand, and they allow a full interpretation of the spectrum.

The interaction between Co^{2+} cations and γ-alumina has also been tackled from a slab model.[53] The calculations show that two Co^{2+} cations can be accommodated in adjacent positions on the surface with a pseudo tetrahedral coordination. Only this structure adequately reproduces all experimental data, with a short Co−Co distance of 3.2 Å in agreement with EXAFS.

5. Catalytic Reactivity of the Surface Organometallic Complexes

Whereas the reactivity of organometallic complexes in homogeneous catalysis is well documented from a theoretical point of view, only a few groups have tackled the study of the reactivity of supported complexes. This is due to the difficulty in combining the representation of the support surface and the calculation of reaction pathways. However, from the development of new methods and of the growing power of computers, such studies have become feasible.

The considered grafted organometallic complexes can be divided into two classes active in two important reactions: the metal hydrides and alkyls involved in hydrogenolysis and alkane metathesis and the metal carbenes involved in alkene metathesis. We will review below these two classes of catalysts and end this part centered on reactivity by a section dealing with alkene polymerization.

5.1. Alkane Hydrogenolysis and Metathesis on Transition Metal Hydrides

Two electron-poor metal hydrides have essentially been considered in the theoretical studies of alkane activation: Ta and Zr. In one case, hydrides of vanadium and niobium have been compared. Finally, the reactivity of an alkyl−tungsten complex has also been reported.

A first series of papers tackles the activation of alkanes on silica-supported group VB metal hydrides and more particularly tantalum hydrides. The silica is represented by a fragment $H_4Si_2O_5(OH)_2$ extracted from the SiO_2 β-cristo-balite structure. Calculations are based on DFT with the B3LYP functional. The first paper deals with σ-bond metathesis of ethane.[54] The key difficulty is to determine the nature and oxidation state of the active surface species. Starting from a bigrafted tantalum(III) monohydride, the following reactions can be envisaged (Scheme 2): the first one involves the cleavage of a C−H bond, then a second ethane molecule reacts with the ethyl−Ta complex to give a methyl−Ta complex and the formation of propane. Finally, the ethyl−Ta complex is regenerated with elimination of methane.

These reactions can occur in two steps, oxidative addition and reductive elimination with formation of a Ta ethyl dihydride intermediate complex, or in a one-step concerted mechanism with a four-center transition state (σ-bond metathesis). None is, however, here satisfactory.

Scheme 2. Potential Mechanisms for the σ-Bond Metathesis of Ethane on Silica-Supported Ta Monohydrides[a]
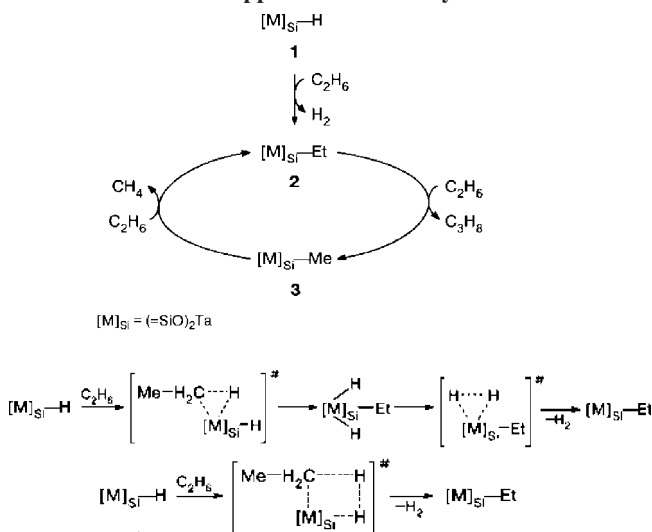
[a] Reprinted with permission from ref 54. Copyright 2003 Springer Science+Business Media.
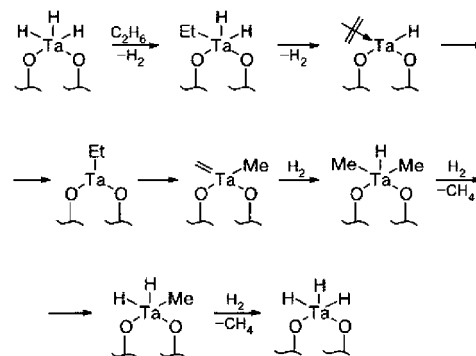
Figure 15. Mechanism for ethane hydrogenolysis involving π-complexes and carbene complexes. Reprinted with permission from ref 55. Copyright 2003 Springer Science+Business Media.

Indeed, on one hand, the transition state for the concerted mechanism could not be detected. On the other hand, the two-step mechanism proceeds by the formation of a dihydride−ethyl complex, more stable than the reaction products by 18 kcal mol^{-1}. The second step and the formation of the products require passing a high barrier, and hence the two-step mechanism is difficult, the reaction being blocked at the intermediate. The mechanism hence remains unresolved at this point.

In the second paper,[55] hydrogenolysis of ethane is explored but this time with a different hydride model, a Ta^V trihydride, because the calculated IR spectrum is in better agreement with the experimental spectrum than the one of the Ta^{III} monohydride (Figure 15). Besides DFT/B3LYP results, MP2 calculations are tested for comparison. The calculation of the reaction pathways demonstrates that ethane hydrogenolysis may proceed by a mechanism involving π-complexes and carbene complexes. The first step, metathesis of a C−H bond giving a dihydride−ethyl Ta complex, is now allowed because the starting point is a more stable Ta trihydride. Hence, the catalytic cycles based on a silica-supported tantalum trihydride can explain the hydrogenolysis activity. The authors propose that this Ta trihydride is also the active site for alkane metathesis, following the two-step mechanism of Scheme 2.

Scheme 3
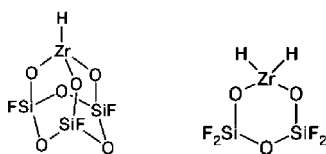
Scheme 4[a]

$$
\begin{array}{cc}
\begin{array}{c} H_b \quad CH_3 \\ | \quad\; | \\ Zr \quad H_a \end{array} &
\xrightleftharpoons[k_{-1}\,;\,E_{a-1}]{k_1\,;\,E_{a1}} &
\begin{array}{c} H_b\!-\!CH_3 \\ \\ Zr\!-\!H_a \end{array} &
\Delta G_1 \quad (1)
\end{array}
$$

$$
\begin{array}{cc}
\begin{array}{c} H_a \quad H_b \\ | \quad\; | \\ Zr \quad H_b \end{array} &
\xrightleftharpoons[k_{-2}\,;\,E_{a-2}]{k_2\,;\,E_{a2}} &
\begin{array}{c} H_a\!-\!H_b \\ \\ Zr\!-\!H_b \end{array} &
\Delta G_2 \quad (2)
\end{array}
$$

$$
\begin{array}{cc}
\begin{array}{c} H_b \quad H_a \\ | \quad\; | \\ Zr \quad CH_3 \end{array} &
\xrightleftharpoons[k_{-3}\,;\,E_{a-3}]{k_3\,;\,E_{a3}} &
\begin{array}{c} H_b\!-\!H_a \\ \\ Zr\!-\!CH_3 \end{array} &
\Delta G_3 \quad (3)
\end{array}
$$

$$
\begin{array}{cc}
\begin{array}{c} H_3C \quad H_a \\ | \quad\;\; | \\ Zr \quad CH_3 \end{array} &
\xrightleftharpoons[k_{-4}\,;\,E_{a-4}]{k_4\,;\,E_{a4}} &
\begin{array}{c} H_3C\!-\!H_a \\ \\ Zr\!-\!CH_3 \end{array} &
\Delta G_4 \quad (4)
\end{array}
$$
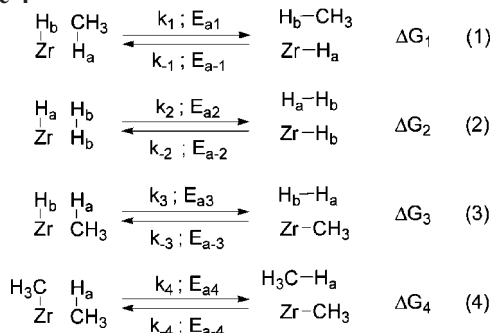
[a] Reprinted with permission from ref 59. Copyright 2003 Wiley−VCH Verlag GmbH & Co. KGaA.

In a third paper, the same group compares the activity of vanadium, niobium, and tantalum hydrides toward metathesis and hydrogenolysis of alkanes.[56] The calculations are conducted at the CASSCF level because the pathways are studied both in triplet and in singlet states. A correct description of the vanadium complexes requires a multiconfigurational approach. A possible role of the triplet states in the reactions catalyzed by niobium and vanadium complexes is pointed out. Indeed, a decrease of the activation energy is observed with these metals due to a crossing between the triplet and singlet paths, which leads to a new low-energy high-spin pathway.

The second type of complexes widely used in alkane activation is constituted by zirconium hydrides. A review article summarizes several works dealing with methane activation and alkane hydrogenolysis.[57] The catalysts are mono- and dihydrides of zirconium supported on silica (Scheme 3). The support is modeled by the small $Si_3O_6F_3$ cluster. F atoms are used instead of OH groups to terminate the cluster. The DFT calculations use the PBE functional and are spin-unrestricted if necessary.

Butane hydrogenolysis is compared on mono- and dihydride catalysts. On the monohydride, the first step is a C−H activation of butane on Zr−H, with elimination of H_2 (σ-bond metathesis). The further step involves a β-ethyl transfer, which is rate determining with a relatively high barrier (31 kcal mol^{-1}). Moreover, the reaction is globally endothermic, which suggests that on the monohydride the reaction cannot occur in mild conditions. On dihydrides, the mechanism is different due to the presence of the second hydrogen atom: from a Zr butyl hydride complex, the β-ethyl transfer still has a high barrier (34 kcal mol^{-1}), but it leads directly to a stable dialkyl complex without passing through the formation of the nonfavorable olefin complex, as it is the case of monohydride. Hence, the hydrogenolysis of butane on dihydrides is feasible at the elevated experimental temperatures (423 K).

A similar conclusion on the better reactivity of the dihydride ($\equiv SiO)_2ZrH_2$ as compared to the monohydride ($\equiv SiO)_3ZrH$ has been reached when modeling silica by a polyhedral silsesquioxane terminated also by fluorine atoms.[58]
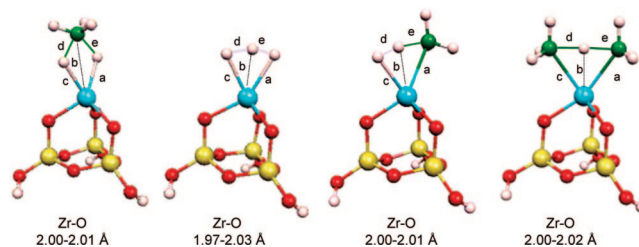
Figure 16. Transition-state geometries for H exchange reactions. Reprinted with permission from ref 59. Copyright 2003 Wiley−VCH Verlag GmbH & Co. KGaA.

The H/D exchange reaction of alkanes has also been studied on grafted ZrH by means of DFT cluster calculations.[59] The silica was represented by the same small cluster as in Scheme 3 but terminated by H instead of F. The PW91 GGA functional was used. Four different pathways were considered (Scheme 4). In each case, the transition state was located and characterized.

All transition states correspond to a metal center surrounded by three ligands in a coplanar arrangement (Figure 16). Their energy depends strongly on the nature and the position of the ligands (H versus CH_3) and varies as follows:

$$ H-H-H \ll H-H-CH_3 < CH_3-H-CH_3 \ll H-CH_3-H $$

Thus, having a hydrogen as the central atom is an important factor for a low-energy transition state.

The main conclusion is that the mechanism for H/D exchange in a CH_4/H_2 mixture does not involve a direct exchange (eq 1) or a methyl exchange (eq 4) but rather a two-step process, C−H activation (eq 3) followed by hydrogenolysis (eq 3). These pathways always allow the use of the transition states with the lowest energy.

The last three studies dealing with the reactivity of supported Zr−H complexes are different in that the support is not represented by small clusters but by surfaces treated with periodic calculation methods. The topic of the first paper is the depolymerization of polyethylene (here modeled by propane) by hydrogenolysis on silica-supported zirconium monohydrides.[60] The (100) and (111) surfaces of β-cristobalite are used as two possible models of a silica surface. The authors consider (2 × 2) and c(4 × 2) unit cells for the (100) and (111) surfaces, respectively. The calculations are based on the Car−Parrinello Molecular Dynamics (CPMD) method with a mixture of localized and plane wave functions.[6] After a study of the surface structures, the grafting of the ZrH_4 complex has been thermodynamically considered. The formation of $SiOZrH_3$ releases 50 kcal mol^{-1}, and the formation of ($\equiv SiO)_3ZrH$ is also exothermic. The depolymerization reaction proceeds in several steps (Figure 17): first, a σ-bond metathesis to attach propane to Zr with liberation of H_2, then a β-alkyl transfer releasing ethylene, model of a polymer one C shorter with a terminal double bond, and finally an insertion of this double bond into a Zr−H bond at another zirconium site. Methane and ethane, the products of the hydrogenolysis reaction, are then formed by σ-bond metathesis with H_2.

An important result for this study is that the formed alkene desorbs and does not remain π-bonded, which avoids a repolymerization. This contrasts with the previous static studies on model clusters where the alkene was remaining adsorbed. A common point, however, is that the C−C cleavage step (β-alkyl transfer) is found to be the rate-limiting one. The nature of the surface is important because the
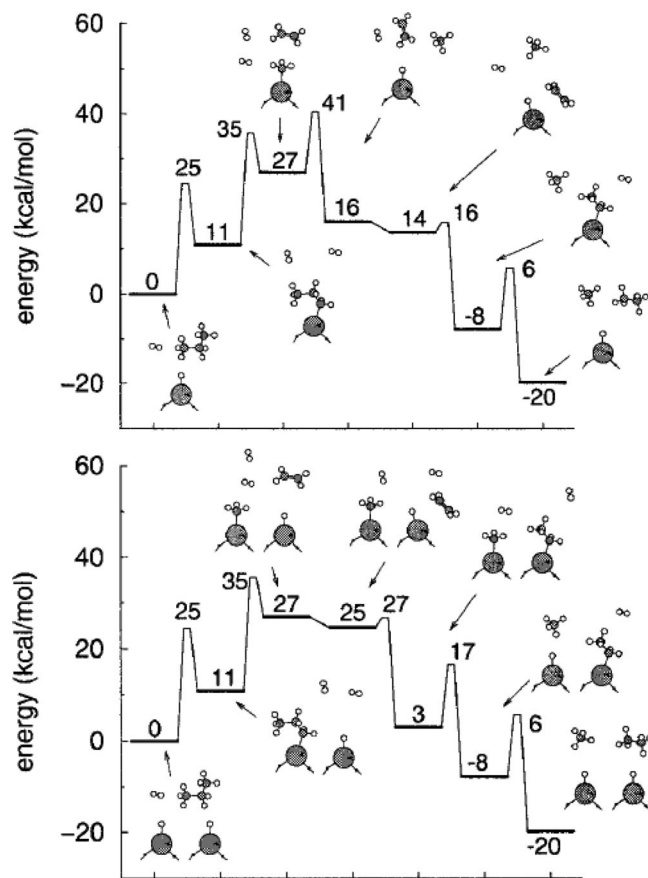
Figure 17. Energy diagram for the hydrogenolysis (depolymerization) of propane on a zirconium monohydride site grafted on a (100) surface (top) and on a (111) surface (bottom) of cristobalite. Reprinted with permission from ref 60. Copyright 2000 American Chemical Society.

barriers for this β-alkyl transfer are 47 and 35 kcal mol^{-1} on the (111) and (100) surfaces, respectively. The barrier on the (100) surface is similar to that previously presented on a cluster model of the Zr monohydride. An important factor is also the coverage in ZrH sites on the surface. If the density of ZrH sites is low, the site on which the β-alkyl transfer occurs must be regenerated by hydrogenolysis before the alkene can react, which requires a supplementary energy barrier. If the ZrH sites are numerous,

a second site can be used for the next steps of the reaction. To summarize, this study underlines the important role of the surface nature and of the density of active sites. It also underlines the importance of a dynamical treatment in the case of weakly bound intermediates.

The two last studies for this hydrogenolysis section differ by the nature of the support, γ-alumina instead of silica. Studies on this support are less common. As described in sections 3 and 4, the interaction of Zr(CH$_2^t$Bu)$_4$ and W($\equiv$CtBu)(CH$_2^t$Bu)$_3$ with γ-alumina leads to well-characterized complexes that can be transformed by hydrogen treatment into hydrides or react with alkanes. The mechanism of formation of alumina-supported zirconium hydrides by treatment of the grafted complex [(AlO)$_2$Zr(CH$_2^t$Bu)$^+$−(CH$_2^t$Bu)Al$^-$] (see Figure 6) with H$_2$ has been investigated by a combined experimental and theoretical study.[61,62] The calculations were performed within the framework of DFT using a periodic description of the system, with the PW91 functional and a plane wave basis set. The surface was modeled by a four-layer slab, the two bottom layers being maintained fixed. A model complex was chosen where the neopentyl ligands were replaced by methyls. The formation of a hydride with elimination of methane occurs from the hydrogenolysis of a Zr−C bond through σ-bond metathesis (Figure 18). In the starting complex, two kinds of CH$_3$ exist, one terminal and one bridging between Zr and Al. The calculations showed that the most favorable pathway starts with the hydrogenolysis of the terminal methyl (barrier of 60 kJ mol^{-1}) and continues with the bridging methyl (barrier of 108 kJ mol^{-1}). The structure of the obtained dihydride, with one terminal and one bridging H, has been evidenced by the match between the experimental and theoretical vibrational spectra.

Experimentally, the formation of the Zr−hydrides is accompanied by the concomitant formation of methane and ethane from hydrogenolysis of the formed neopentane. As a model, hydrogenolysis of butane has been studied with this alumina-supported zirconium hydride. The first step is the C−H activation of butane by σ-bond metathesis. Several pathways were compared depending on the position of the activated C−H bond, at a primary or secondary carbon. The reaction then proceeds through a β-alkyl transfer that requires a high barrier of 135 kJ mol^{-1}, similar to the one found on
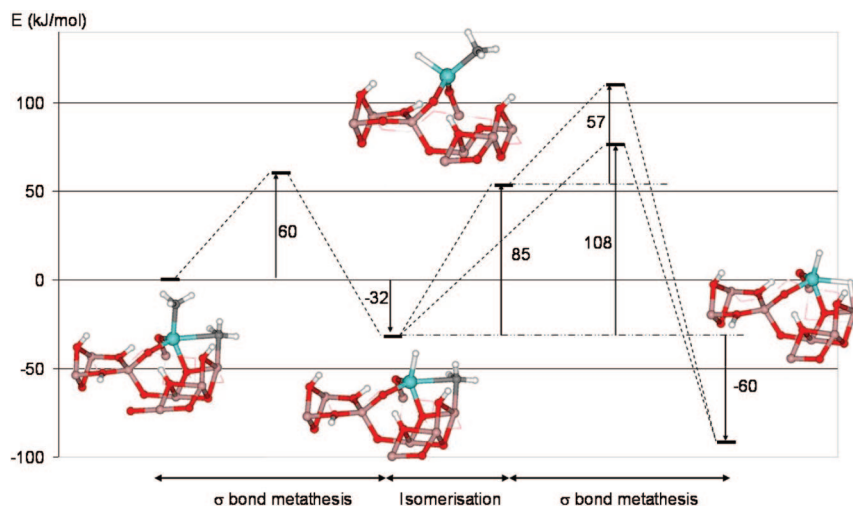
Figure 18. Reaction path for the formation of [(AlO)$_2$Zr(H)(μ-H)Al]. Energies in kJ mol^{-1}. Reprinted with permission from ref 61. Copyright 2007 American Chemical Society.

Scheme 5. First Hypothesis for Propane Metathesis on $(AlO)W(\equiv C^tBu)(CH_2{}^tBu)_2{}^a$
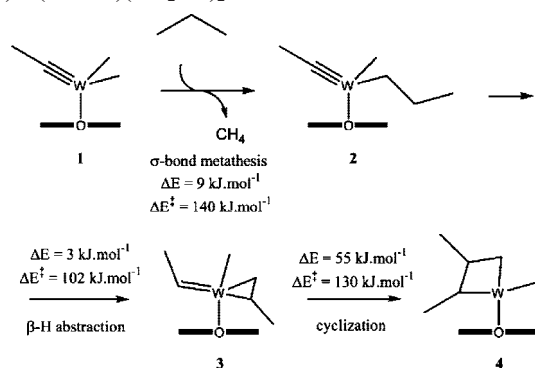
silica.[57,60] Hence, the β-alkyl transfer is also the rate-determining step on alumina support as it is on silica.

The monoaluminoxy complex $(\equiv AlO)W(\equiv C^tBu)$ $(CH_2{}^tBu)_2$, formed by the interaction of $[W(\equiv C^tBu)(CH_2{}^tBu)_3]$ on partially hydroxylated γ-alumina, is active in propane metathesis. Olefin metathesis has been proposed as the key process in alkane metathesis, because olefins have been identified as primary products. The mechanism for the initial alkane dehydrogenation step to form olefins has been studied by means of DFT periodic calculations.[63] The method was the same as in the previous study; in the model complex, the neopentyl ligands were replaced by methyls and ($\equiv C^tBu$) by ($\equiv CMe$). The activation of propane by the grafted complex can proceed in three steps (see Scheme 5): the first one is a C–H/ W–C σ-bond metathesis and is highly activated (140 kJ mol^{-1}). The second step is a β-H abstraction by the carbyne ligand and leads to a carbene and a coordinated olefin on W^{IV}. The formation of a metallacyclobutane, central intermediate for olefin metathesis, can then occur, yielding a d^2 complex with a high barrier (130 kJ mol^{-1}).

The activation barriers of this process are too high, particularly if the entropic effects are introduced, to account for the experimental results. However, it has been shown by a combined theoretical and experimental study that the hydroxylated surface of γ-Al$_2$O$_{3-500}$ presents defects (as dehydroxylated Al^{III} atoms) that can activate H$_2$ and CH$_4$.[64] Such activation can be applied to propane: one C–H bond of propane interacts with a tricoordinated Al atom with a low barrier (25 kJ mol^{-1}) to give an alkyl–aluminum. Propene is then obtained by β-H elimination with a high barrier (140 kJ mol^{-1}) that can be reduced if entropy is taken into account. The main conclusion of this study is that the support can have a direct chemical role and take part in the reaction.

The next step of the whole process, the metathesis of the formed propene, will be discussed in the next part devoted to olefin metathesis.

5.2. Olefin Metathesis

While many theoretical investigations of the olefin metathesis reaction have been reported at the molecular level, modeling homogeneous catalysis, only a few theoretical studies have been undertaken for reactions proceeding in heterogeneous catalysis, with complexes supported on a surface. In a way at the frontier between the two approaches, a first set of studies considers molecular complexes but with a siloxy OSiH$_3$ ligand to represent a silica surface. The

Scheme 6. Active Site and Molybdacyclobutane Intermediates for Olefin Metathesis on an Oxo–Carbene–Molybdene Complex Grafted on Alumina^a

Mo^{VI} methylidene   TBP molybdacyclobutane   SP molybdacyclobutane
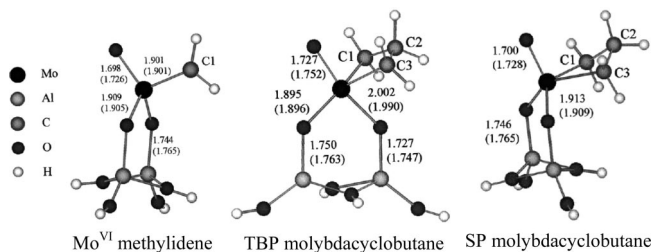
chosen reaction is ethylene metathesis with d^0 Schrock-type catalysts $M(\equiv ER^1)(=CHR^2)(X)(Y)$. In the first paper,[65] the catalyst is the Re alkylidyne complex Re($\equiv C^tBu$)- $(=CH^tBu)(X)(Y)$. A key step of the mechanism is the structural preparation of the catalyst for the coordination of ethylene. The associated barrier depends on the nature of X and Y. It is the smallest when X is a good σ-donor and Y a poor one. This explains the high efficiency of the silica-supported system Re($\equiv C^tBu$)($=CH^tBu$)(CH$_2{}^tBu$)(OSi$\equiv$) as compared to its homogeneous equivalent Re($\equiv$CMe)- $(=CHMe)(OR)_2$. In the second paper,[66] several metals are compared (Re, Mo, W). In all cases, the catalysts are more efficient when they are unsymmetrical (X $\neq$ Y). However, in the case of W or Mo, the OSiH$_3$ group does not give the same barrier decrease as in the case of Re. This means that grafting the W or Mo catalyst on silica would not improve the reaction rate. In the last paper of the series,[67] the authors aim at explaining the deactivation of the surface complex Re($\equiv C^tBu$)($=CH^tBu$)(CH$_2{}^tBu$)(OSi$\equiv$) observed experimentally. This deactivation starts by a β-H transfer trans to the weak σ-donor ligand (siloxy) at the intermediate metallacyclobutane. The most accessible pathway then proceeds with the insertion of ethylene in the Re–H bond followed by α-H abstraction yielding byproducts or β-H abstraction leading to degrafting. The calculated barriers are in the same range as that of the metathesis reaction, which explains the formation of the byproducts as primary products and the rapid deactivation of the catalyst.

Let us now switch to more realistic models of the solid support. The series of papers by Handzlik and co-workers deals with olefin metathesis catalyzed by molybdenum complexes supported on alumina or silica. The first articles are based on cluster calculations and the last ones on periodic calculations. In the first three studies, very small Al$_2$(OH)$_6$ model clusters were used for representing the alumina support, and the active center was a Mo methylidene. The DFT calculations were carried out with the B3LYP exchange correlation functional. The comparison of Mo^{VI} and Mo^{IV} methylidene in alkene metathesis leads to the conclusion that the Mo^{IV} centers are not active because of a high energy barrier for the formation of the intermediate metallacyclobutane (singlet case) or a too high stability of this intermediate (triplet case).[68] Hence, only Mo^{VI} centers are considered in the further studies. The addition of ethene to the molybdenamethylidene leads to a molybdacyclobutane with a trigonal bipyramid (TBP) geometry, which can rearrange, by a Berry pseudorotation, to the more stable complex with a square pyramidal (SP) geometry[69] (see Scheme 6).

No transition state could be localized directly connecting the reactants and the SP cyclobutane. Hence, the metathesis

Scheme 7. Two Possible Grafted Sites for Molybdene−Oxo−Carbene Fragment on the (100) Surface of Alumina, Modeled by a Cluster[a]
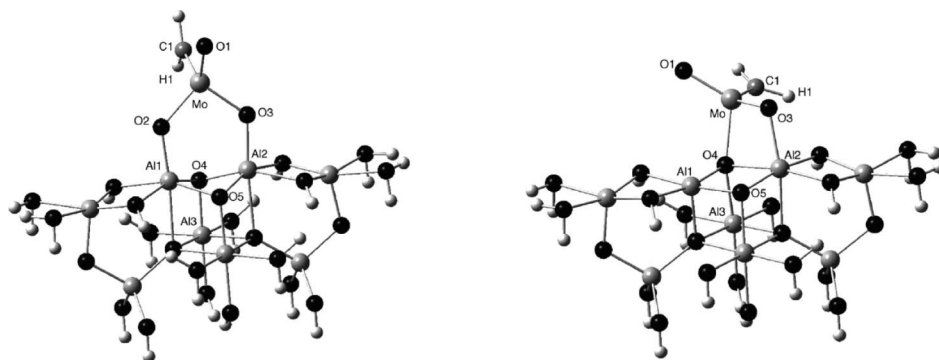
[a] Reprinted with permission from ref 72. Copyright 2005 Elsevier.

reaction must involve the TBP complex as intermediate. The free energy barrier for the TBP-SP rearrangement and the one for the TBP cyclobutane decomposition into ethylene and molybdenamethylidene, the second step of the metathesis reaction, are calculated at similar values ($\Delta G^{\ddagger} \approx 36$ kJ mol^{-1}). Hence, the two reactions are in competition, and the exothermic rearrangement TBP-SP decreases the overall rate of ethene metathesis. The same conclusion has been reached for propene metathesis[70] that leads to ethylene and 2-butene. In this case, the catalytic cycle must be continued by propene addition to the formed Mo−ethylidene species, for which the barrier is a little lower than for propene addition to Mo−methylidene. The cross-metathesis of ethene and 2-butene has also been studied. The activation energies depend on the length of the alkene and of the nature of the Mo−alkylidene center. The conclusion of this series of works is that, insofar as the small cluster models are reliable, the rate of alkene metathesis is slowed by the TBP-SP transformation of the intermediate metallacyclobutane.

It is known experimentally that the activity of heterogeneous Mo catalysts strongly depends on their structure. Hence, the metathesis activity toward propene of monomeric Mo-methylidene centers has been compared on two different surfaces of γ-alumina: (100) and (110).[71] The same method as before was used, but the clusters are larger and hence they represent better the surface structure. Two differences have been found between the two surfaces. The first one concerns the formation of the molybdacyclobutane: on the (100) surface it is formed directly, whereas on the (110) surface a propene π-complex is obtained because of the reduced electron density on molybdenum. The second difference is that the TBP conformation of the molybdacyclobutane is more stable than the SP one on the (110) surface. It results that the (110) surface has a better catalytic activity in alkene metathesis. This study shows the influence on the reactivity of the support nature and of the stability of the intermediates.

Another important factor is also the nature of the grafting site.[72] The Mo−methylidene moiety can replace two terminal hydroxyl groups on octahedral aluminum atoms (Scheme 7, left), as it is the case in the papers commented above, or replace only one terminal hydroxyl and be coordinated directly to a bridged oxygen of alumina (Scheme 7, right).

As in the previous paper, a π intermediate complex is formed in the case of the latter grafted complex, because of a reduced electron density on molybdenum, which results in a pathway with moderate energy barriers. Hence, the site

Scheme 8. Degenerate Metathesis
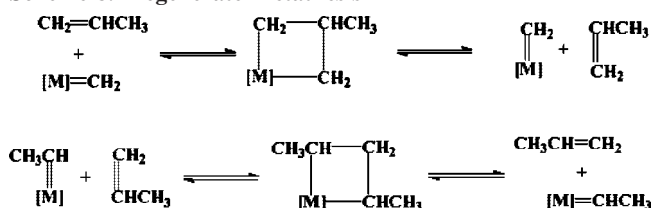
where Mo is grafted to a bridged oxygen has a better metathesis activity.

It is known that productive metathesis is always accompanied by so-called degenerate metathesis that gives back the starting reactant. It has been observed experimentally that degenerate metathesis on heterogeneous molybdenum systems proceeds faster than the productive one (Scheme 8). This problem has been addressed by comparing the activity of [Mo]=CH$_2$ and [Mo]=CHCH$_3$ on small Al$_2$(OH)$_6$ models.[73]

The conclusion is that the degenerate metathesis is indeed favored over the productive one if Mo−ethylidene centers are considered. However, this is not true for the Mo−methylidene sites.

Until now, monomeric Mo centers have been studied. In the next paper, dimeric Mo centers are considered and compared to monomeric ones, always with the same cluster models.[74] The dimeric Mo centers are found more active in alkene metathesis because the cyclo-reversal step leading to the products of metathesis is preferred over the isomerization of the TBP metallacyclobutane into the SP form.

Finally, the same mechanism has also been studied for Mo−alkylidene centers grafted on silica, modeled by clusters.[75] The main feature is that the transformation of the TBP molybdacyclobutane into the SP conformation is kinetically unfavorable, whatever the considered site, which explains the high activity in metathesis of the Mo−alkylidene complexes grafted on silica, by comparison with alumina.

The conclusion of this series of studies about alkene metathesis with molybdenum complexes is that the efficiency of the catalyst depends on two main factors: the ability of the complex to make a π-adduct with the alkene and the feasibility of the transformation between the TBP and SP forms of the intermediate molybdacyclobutane, which competes with the direct metathesis pathway.

The last study on the same catalytic system is based on a different approach because the calculations are periodic.[76,77] The use of an alumina surface instead of clusters allows for the exploration of more numerous grafting sites and
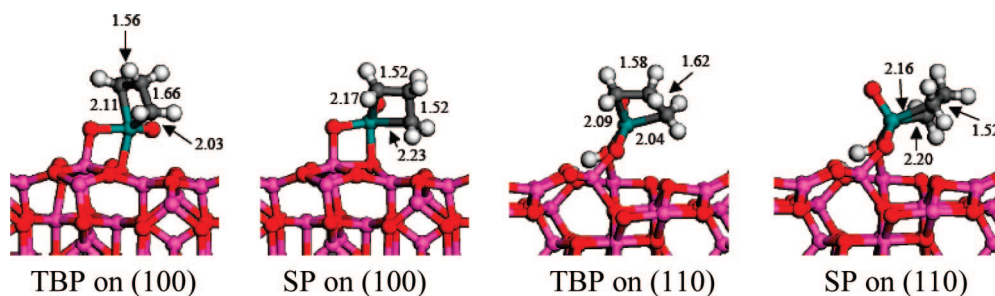
Figure 19. Structure of the TBP and SP metallacyclobutane intermediate with Mo−methylidene species grafted on a periodic model of γ-alumina. Reprinted with permission from ref 76. Copyright 2008 Elsevier.
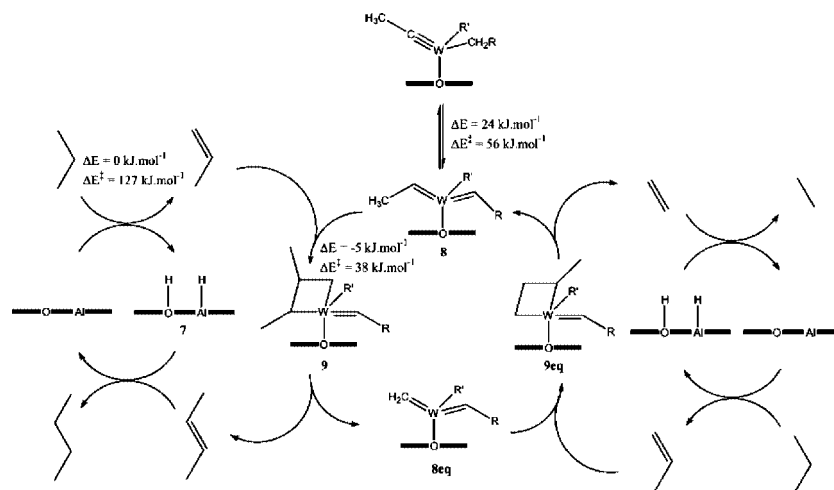
Figure 20. Proposed mechanism for butane metathesis on a W alkyl carbyne complex grafted on alumina, including dehydrogenation/hydrogenation on the support and olefin metathesis on the supported complex. Reprinted with permission from ref 63. Copyright 2007 Elsevier.

imposes constraints to the structure of the species involved in the mechanism. The DFT calculations are performed with the PW91 functional and a plane wave basis set. Two surfaces of γ-Al$_2$O$_3$ are compared, (100) and (110). A first result is that the Mo−methylidene species are more stable on the (110) than on the (100) surface. The same intermediates are investigated as for the cluster calculations, the π-complex of ethylene and the metallacyclobutane (see Figure 19).

The calculation of the Gibbs free energy leads to the conclusion that the relative stability of the different Mo−methylidene species varies with temperature and water vapor pressure. Their activity in alkene metathesis strongly depends on their geometry and location on the γ-Al$_2$O$_3$ surface. As it is the case with the cluster models, the TBP and SP molybdacyclobutane intermediates are found decisive for the efficiency of the catalyst. In many cases, these species are more stable than the reactants, and hence their opening to restore carbene and olefin is the rate-limiting step of olefin metathesis. The large majority of sites are blocked at the molybdacyclobutane step, and their catalytic activity is small. The species active at low temperature has a reduced stability because of constraint imposed by the surface that deforms the Mo environment as compared to a coordination complex. Therefore, the key result of this study is that the various described Mo species show a very different activity, as a function of the constraints imposed by the grafting to the solid support. Hence, only a small fraction of the Mo sites are active. To produce efficient catalysts, the grafting process has therefore to be chemically controlled.

Olefin metathesis also been has been proposed recently as the central step for the carbon−carbon bond formation process in alkane metathesis, the transformation of a given alkane into its higher and lower homologue. In that context, the mechanism of ethylene metathesis has recently been studied on a Ta−hydride−carbene complex grafted on a small molecular model of silica.[78] A low-energy pathway is found, hence underlining the possibility to follow olefin metathesis pathway within the alkane metathesis mechanism. One originality of this system is that the standard direct metathesis pathway with [2 + 2] addition and cycloreversion steps is forbidden, because it would require passing through a high energy intermediate with the carbene trans to the hydride. The pathway involves several low-energy steps of rearrangement of the metallacyclobutane, to avoid that configuration.

Similarly, propene metathesis has been proposed as the central step for the propane metathesis mechanism on (≡AlO)W(≡C^{t}Bu)(CH$_2^t$Bu)$_2$ (see section 5.1).[63] The whole catalytic cycle is given in Figure 20.

To obtain the carbene required for metathesis, the carbyne ligand isomerizes to a bis-carbene with a small barrier (56 kJ mol^{-1}). The rest of the mechanism then proceeds with low barriers, in contrast to the direct propane metathesis (Scheme 5). The reason is that, in propane metathesis, the metallacycle is a d^2 complex of W^{IV}, whereas, in propene metathesis, the metallacycle is a more stable d^0 complex of W^{VI}. Hence, these results confirm the hypothesis that olefin metathesis is the central process in alkane metathesis.

5.3. Polymerization

One first example in this domain is the mechanistic study of ethylene polymerization on silica-supported zirconium
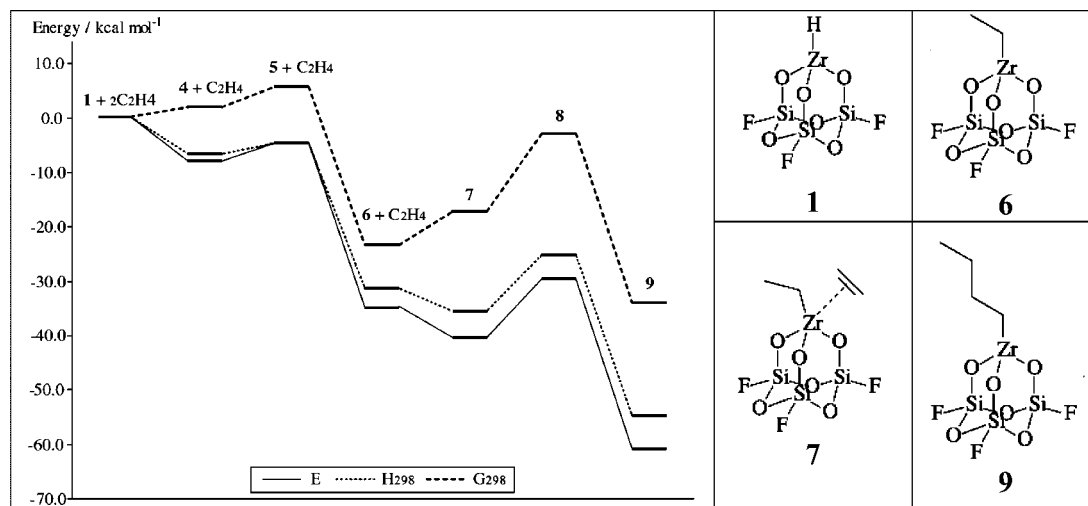
Figure 21. Reaction energy, free energy profiles (at 298 K), and structure of intermediates for ethylene polymerization on grafted Zr–H species. Reprinted with permission from ref 54. Copyright 2003 Springer Science+Business Media.

hydrides $(\equiv SiO)_3ZrH$ and $(\equiv SiO)_2ZrH_2$ (Figure 21).[54] The support is represented by a very small cluster $Si_3O_6F_3$, and the calculations are performed with the PBE functional. The first step of the reaction involves insertion of ethylene into the Zr–H bond, and then the chain grows by successive insertions into the newly formed Zr–C bonds. The rate of ethylene polymerization is found to be very similar if the monohydride or the dihydride is considered as the active site. In both cases, the reaction is easy with barrier in free energy not exceeding 20 kcal mol^{-1}.

Ethylene polymerization reactivity has been also explored by Marks et al.[51] on $Cp_2ZrCH_3^+$ adsorbed on dehydrated alumina. Two adsorption sites of the cation are compared (on a μ_2 or on a μ_3 O atom on alumina), and the polymerization activity is compared to that of the homogeneous catalyst. The activity is correlated with the energy of the ethylene π-complex formation. The two surface cationic complexes give a different reactivity, only the least stable one being highly active (more than the homogeneous analogue). This is in good agreement with experimental data, which indicates that only a fraction of the Zr sites on alumina are active.

The next two studies do not involve organometallic complexes. They can nevertheless be related to surface organometallic catalysis because the initiation step is the formation of a metal–alkyl bond giving the reactive complex.

The first study deals with ethylene polymerization catalyzed by a pseudotetrahedral mononuclear $Cr(II)/SiO_2$ site.[79] The calculations are based on DFT, and the catalyst is modeled by small silicachromate clusters. The initiation step, shown in Figure 22, is supposed to be the formation of either an ethenylhydridochromium(IV), an ethylidenechromium, or a chromacyclopentane from the interaction of one or two ethylene molecules.

From these species, several starting points for polymerization are derived and compared for the propagation phase. The first conclusion is that chromacyclopentane, obtained by fixation of two ethylene molecules, is the dominating initial species. Chain growth proceeds through direct ethylene insertion into a Cr–C bond with a large barrier of 119 kJ mol^{-1} (Figure 23). Experimentally, the formation of 1-alkene in the early stage of the reaction is reported. From the formed chromacycloalkane, a β-H transfer to the α carbon at the other end of the carbon chain leads to a coordinated alkene.
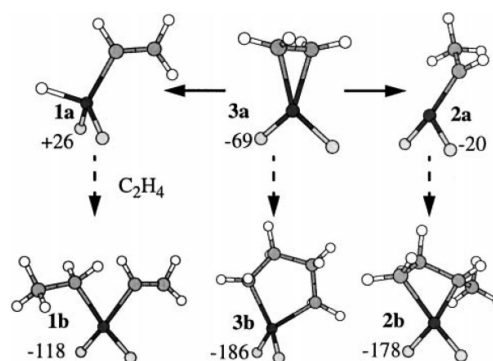
Figure 22. Initiation step for ethylene polymerization on model $Cr(II)/SiO_2$. Energies in kJ mol^{-1} relative to free complex and ethylene. Reprinted with permission from ref 79. Copyright 2000 Elsevier.

This reaction is in competition with the growth of the chain by further insertion of ethylene into the chromacycloalkane and shows a slightly smaller barrier (98 kJ mol^{-1}), hence explaining the formation of 1-alkene. The barrier for ethylene insertion into this cyclopentane (119 kJ mol^{-1}) is too high to explain the polymerization. A key factor to control the barrier seems to be the OCrO angle between the chromate and the siloxanes, which means here again that the strain induced by the support plays an important role.

In a second paper by the same authors,[80] two other mononuclear Cr(II) sites are considered: a highly strained pseudo-octahedral and a pseudotetrahedral with a supplementary coordinating silanol group. With a pseudo-octahedral site, the barrier for ethylene insertion is largely reduced but not enough to be competitive with the release of small alkenes. In contrast, the pseudotetrahedral site assisted by a vicinal silanol seems to be a good precursor for polymerization: a hydrogen transfer occurs from the silanol to form a four-coordinated ethylchromium(IV) species on which subsequent insertion of ethylene proceeds with a modest barrier. Nevertheless, the best model cluster found for interpreting the polymerization of ethylene by the Cr/SiO_2 system is a Cr dinuclear site,[81] due to a low insertion barrier.

The comparison of these three articles shows the importance of the environment of the active site: ligand field of the metal and participation of the surface to the reaction. Nevertheless, the small size of the clusters simulating the surface could introduce spurious effects and allows geom-
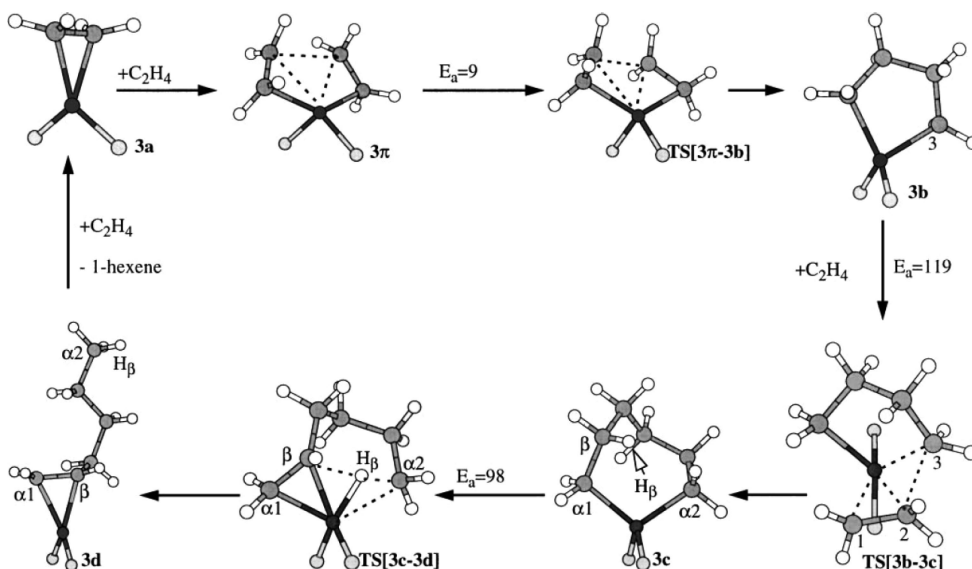
Figure 23. Stationary points along the reaction path of 1-hexene formation on model Cr(II)/SiO$_2$. Activation energies in kJ mol^{-1}. Reprinted with permission from ref 79. Copyright 2000 Elsevier.
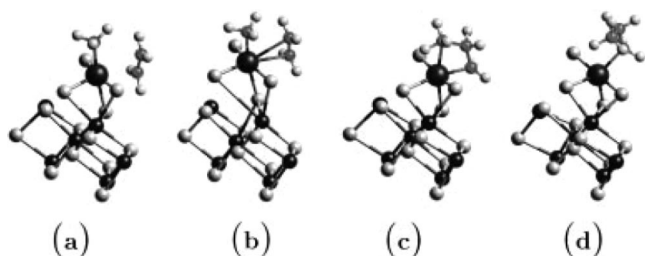
Figure 24. Most important steps in the insertion reaction for the 5-fold site in the case of Ziegler−Natta polymerization of ethylene with titanium active sites supported on the (110) surface of MgCl$_2$: the ethylene approach (a), the π-complex formation (b), the transition state (c), and the formed chain (d). Reprinted with permission from ref 82. Copyright 1998 American Chemical Society.

etries for approaching ethylene that are not realistic on a real surface.

The second topic concerns the Ziegler−Natta polymerization of ethylene with titanium active sites supported on the (110) surface of MgCl$_2$.[82] The method used is totally different from the previous one because the study is based on DFT periodic molecular dynamics using the Car−Parrinello scheme (CPMD). Nevertheless, as previously, the initiation step requires the pre-existence of a metal−carbon bond and of an under-coordinated site (Ti(IV)). Two different configurations are compared for titanium. In both, Ti is surrounded by four Cl and one CH$_3$ ligands but in different geometries. The barriers for ethylene insertion are calculated to be low (13−15 and 7 kcal mol^{-1}, respectively), which can be explained by the formation of an agostic interaction between Ti and one H of the methyl group that reduces the steric hindrance with the approaching ethylene. The best site is a 5-fold site in which one Cl atom bound to Ti has no bond with the substrate and can easily be displaced, allowing the alkene to approach (see Figure 24). Hence, the reactivity depends on the local geometry.

The further step of the mechanism, the insertion of a second ethylene, has also been investigated, starting from (d) in Figure 24. The ethylene coordination requires a large displacement of the chain, which orientates parallel to the surface. The reaction then proceeds with the same low-energy

barrier as for the first ethylene molecule and is also agostic-assisted. This work therefore depicts a realistic pathway for explaining the polymerization of alkenes by the Ziegler−Natta catalysts and provides support for the agostic-assisted insertion of alkenes in the Ti−C bond. The results compare well with those of calculations done on nonsupported Ti catalysts.[83]

In a second paper by the same authors, the problem of isotacticity is addressed with the same method as previously.[84] The polymerization of propene is studied with the same Ti catalyst on MgCl$_2$ (110). On the 5-fold catalytic center, propene can approach only with CH$_3$ far from the substrate. For the approach of a second propene molecule, several geometries are tested. One of them, where propene inserts into the Ti−CH$_3$ bond in the same position as for the first insertion, leads to stereoselectivity. In this case, the barrier is the lowest among all possible situations (10.5 kcal mol^{-1}), and the insertion is α-agostic assisted. It is clear that the resulting stereoselectivity is a consequence of the local geometry of the active site.

Finally, a comparison between various surfaces of MgCl$_2$, (100), (110), and (104), and between mononuclear, as studied before, and binuclear complexes is made in a third study.[85] After having studied the structure of the three surfaces, the authors investigate the grafting of TiCl$_4$ and Ti$_2$Cl$_6$ precursors of the alkyl−Ti complexes needed for polymerization. Stable TiCl$_4$ adducts are allowed only on the (110) surface where Mg atoms have a low coordination. In contrast, Ti$_2$Cl$_6$ binds to the (100) surface with five bonds. To test the ability of this binuclear complexes to achieve polymerization, the alkylated center is simulated by substituting one Cl with an isobutyl group. During the complexation of propene on one of the Ti atoms, a disruption of the dinuclear species is observed with the other TiCl$_4$ moiety being expelled. The active Ti loses also some bonds with the substrate and becomes Ti(II). The same conclusion is reached if the calculations are done on the triplet states. Hence, dinuclear species do not remain stable during polymerization.

The conclusion of these studies on Ziegler−Natta catalysts is that the only active site is a mononuclear complex grafted on the (110) surface with a 5-fold configuration allowing flexibility. These results indicate that the consideration of

the surface in the calculations is essential and show that the use of small cluster models can be insufficient to take into account the complexity of the Ziegler–Natta catalysts.

6. Conclusion

The various theoretical studies exposed in this Review bring several types of insights on surface organometallic complexes: mechanism of formation, nature of bonding with the surface, structure of the surface organometallic complex, interpretation of spectroscopic data, nature of reaction intermediates, and finally catalytic reactivity. Their contribution is especially important when combined with adequate experimental data. The association with EXAFS gives a direct input on the structure. Other spectroscopic techniques such as IR or NMR play also a central role, because they establish a link between the reality of the experimental system (in conditions as close as possible to the catalysis ones) and the virtual world of models. The simulations of the spectra are nowadays developing quickly, which gives a direct (and nonforgiving) test of the theoretical models against the experimental spectra. For the reactivity, theory has the major advantage to propose, after computer intensive simulations, a microscopic view of the mechanism. A simulation of the reaction kinetics based on this energy profile from first principles allows again the confrontation with the experiment.

Concerning surface organometallic chemistry, one of the key questions is whether the grafted complex is electronically similar or different as compared to the related molecular complex. Can unprecedented catalytic properties be obtained? Contrasting answers are proposed. In some cases, it is claimed that the oxide support (as silica) is just a ligand similar to any alkoxy-ligand, nothing special. This is the case if monopodal complexes are considered, as obtained, for example, for the silica-supported olefin metathesis catalyst $[(\equiv SiO)Re(\equiv CR)(\equiv CHR)(CH_2R)]$ (R = Me and R = ^tBu). In contrast, for dipodal coordinations and higher, the rigidity of the surface "ligand" is an important aspect, imposing constraints on the grafted complex especially on the angles around the metal. These constraints will destabilize the grafted complex, and hence make it intrinsically more reactive than the homogeneous counterpart. Surface organometallic chemistry might hence produce a well-controlled species, which is electronically different from the molecular precursor and that can exist as isolated molecular species. In contrast, a simple grafting by a ligand, with no direct metal–surface interactions, cannot produce this effect. Such constraints can also be obtained, however, by large polydentate ligands, but their rigidity is reduced as compared to the surface.

The stability of the active site is also an important aspect for catalysis. In solution, the electron-deficient complexes can meet, dimerize, and hence deactivate. When grafted on the support, such dimerization is impossible, which is an important indirect aspect for the reactivity of the grafted system. If not intrinsically more active, the surface organometallic complex can become more stable and have a longer lifetime.

Another recurrent question is whether or not single sites are produced. Cases of true single sites are indeed rare. Comparison of various grafting modes, for example, for CH_3ReO_3 or molybdena on alumina, underlines cases where a mixture of sites, and not a single site, is obtained with only one being highly active. In such systems, the ultimate goal of surface organometallic chemistry is not attained because only a small fraction of the metal atoms are active. In such cases, the majority surface species, which is the one seen by spectroscopy, is not responsible for the catalytic event. There is a strong added value of modeling in such cases, because various species, including slightly less stable ones, can be explored and compared, but the link with experimental characterization is more difficult.

The next frequently asked question is about the influence of the support. Will a different structure and reactivity be obtained if silica, alumina, or zirconia is used? Theory gives key answers on the role and differences between supports. Silica and alumina are often used, and sometimes can give markedly different results. Both supports present, for example, OH groups enabling the grafting of alkyl complex. Alumina, however, presents a richer chemistry. The theoretical studies have shown that it can play a dual role, as a support and as a Lewis acid cocatalyst. Indeed, it can form, in addition to the covalent link, an ion pair with a cationic metal center showing an enhanced electrophilic character, as in the case of Zr. This explains why the Zr–alkyl complex supported on alumina is active for olefin polymerization, while it is inactive on the silica support, except if Lewis acid cocatalysts are used. In other cases, a direct chemical role of the support is involved because the catalyst activation step occurs on the support. Finally, just changing the structure of the support ((100) vs (110) surface for β-cristobalite as a model of silica) can change the reactivity of the grafted complex.

On more fundamentals aspects, theory brings important and new insights on the elementary mechanisms, explaining the formation of the surface complex. In some cases, various possible pathways (as σ bond metathesis and addition) can be discriminated, and this is important for the design of new grafting modes. Theory can also define reactivity indexes, which allow the comparison of various systems for their potential reactivity, without undertaking the tedious task to explore all reaction mechanisms. It can also probe the importance of the spacing between the grafted complexes, hence explaining the influence of loading. Two neighboring sites can be involved in the reaction at high loading, which is a specific aspect of surface organometallic chemistry.

Simulation of structure and reactivity related to surface organometallic chemistry is a young research field. Large perspectives are opened. The pertinence of the approach lies in the combination of methods: theory, spectroscopy, structure, reactivity. A strong coupling with kinetics and with in situ spectroscopic techniques is essential to understand such catalysts in conditions close to the catalytic ones. Experiment and simulations could be extended to other spectroscopic techniques such as Raman, able to probe the bonds between the complex and the surface, or NEXAFS. In situ NMR is also a technique of choice. For the simulation techniques, hybrid methods will certainly develop due to their ability to describe large systems from a combination of two levels of theory, a precise one for the metallic complex and a less accurate one for the environment and the rest of the support. This will allow the study of catalysis in realistic conditions.

7. References

(1) Copéret, C.; Chabanas, M.; Petroff Saint-Arroman, R.; Basset, J.-M. *Angew. Chem., Int. Ed.* **2003**, *42*, 156.
(2) Cornils, B.; Herrmann, W. A. *Applied Homogeneous Catalysis with Organometallic Compounds*, 2nd ed.; Wiley–VCH: New York, 2002; Vol. 1.

(3) Cornils, B.; Herrmann, W. A. *Applied Homogeneous Catalysis with Organometallic Compounds*, 2nd ed.; Wiley−VCH: New York, 2002; Vol. 2.

(4) Guzman, J.; Gates, B. C. *Dalton Trans.* **2003**, 3303.

(5) Fierro-Gonzalez, J. C.; Kuba, S.; Hao, Y.; Gates, B. C. *J. Phys. Chem. B* **2006**, *110*, 13326.

(6) van Santen, R. A., Sautet, P., Eds. *Computational Methods in Catalysis and Materials Science*; Wiley−VCH: Weinheim, 2009.

(7) Helgaker, T.; Jorgensen, P.; Olsen, J. *Molecular Electronic-Structure Theory*; Wiley: Chichester, 2004.

(8) Parr, R. G.; Yang, W. *Density-Functional Theory of Atoms and Molecules*; Oxford University Press: New York, 1989.

(9) Morokuma, K.; Maseras, F. *J. Comput. Chem.* **1995**, *16*, 1170.

(10) Hoffmann, R. *Rev. Mod. Phys.* **1988**, *60*, 601.

(11) Kresse, G.; Furthmueller, J. *Phys. Rev. B* **1996**, *54*, 11169.

(12) Segall, M. D.; Lindan, P. J. D.; Probert, M. J.; Pickard, C. J.; Hasnip, P. J.; Clark, S. J.; Payne, M. C. *J. Phys.: Condens. Matter* **2002**, *14*, 2717.

(13) Pisani, C.; Dovesi, R.; Roetti, C. *Hartree-Fock Ab-initio of Crystalline Systems, Lecture Notes in Chemistry*; Springer Verlag: Heidelberg, 1988; Vol. 48.

(14) Pisani, C.; Maschio, L.; Casassa, S.; Halo, M.; Schütz, M.; Usvyat, D. *J. Comput. Chem.* **2008**, *29*, 2113.

(15) Ditchfield, R. *J. Chem. Phys.* **1972**, *56*, 5688.

(16) Pickard, C. J.; Mauri, F. *Phys. Rev. B* **2001**, *63*, 245101.

(17) Jónsson, H.; Mills, G.; Jacobsen, K. W. In *Classical and Quantum Dynamics in Condensed Phase Simulations*; Berne, B. J., Ciccotti, G., Coker, D. F., Eds.; World Scientific: Singapore, 1998; p 385.

(18) Boero, M.; Parrinello, M.; Terakura, K. *J. Am. Chem. Soc.* **1998**, *120*, 2746, and references herein.

(19) Haukka, M.; Hirva, P. *Surf. Sci.* **2002**, *511*, 373.

(20) Sinclair, P. E.; Sankar, G.; Catlow, C. R.; Thomas, J. M.; Maschmeyer, T. *J. Phys. Chem. B* **1997**, *101*, 4232.

(21) Räty, J.; Suvanto, M.; Hirva, P.; Pakkanen, T. A. *Surf. Sci.* **2001**, *492*, 243.

(22) Moses, A. W.; Ramsahye, N. A.; Raab, C.; Leifeste, H. D.; Chattopadhyay, S.; Chmelka, B. F.; Eckert, J.; Scott, S. L. *Organometallics* **2006**, *25*, 2157.

(23) Salameh, A.; Joubert, J.; Baudouin, A.; Lukens, W.; Delbecq, F.; Sautet, P.; Basset, J.-M.; Copéret, C. *Angew. Chem., Int. Ed.* **2007**, *46*, 3870.

(24) Digne, M.; Sautet, P.; Raybaud, P.; Euzen, P.; Toulhoat, H. *J. Catal.* **2002**, *211*, 1.

(25) Digne, M.; Sautet, P.; Raybaud, P.; Euzen, P.; Toulhoat, H. *J. Catal.* **2004**, *226*, 54.

(26) Joubert, J.; Fleurat-Lessard, P.; Delbecq, F.; Sautet, P. *J. Phys. Chem. B* **2006**, *110*, 7392.

(27) Joubert, J.; Delbecq, F.; Sautet, P.; Le Roux, E.; Taoufik, M.; Thieuleux, C.; Blanc, F.; Copéret, C.; Thivolle-Cazat, J.; Basset, J. M. *J. Am. Chem. Soc.* **2006**, *128*, 9157.

(28) Machado, E.; Kaczmarski, M.; Ordejón, P.; Garg, D.; Norman, J.; Cheng, H. *Langmuir* **2005**, *21*, 7608.

(29) Barker, C. M.; Gleeson, D.; Kaltsoyannis, N.; Catlow, C. R. A.; Sankar, G.; Thomas, J. M. *Phys. Chem. Chem. Phys.* **2002**, *4*, 1228.

(30) Sinclair, P. E.; Catlow, C. R. A. *J. Phys. Chem. B* **1999**, *103*, 1084.

(31) Fraile, J. M.; Garcia, J. I.; Mayoral, J. A.; Salvatella, L.; Vispe, E.; Brown, D. R.; Fuller, G. *J. Phys. Chem. B* **2003**, *107*, 519.

(32) Espelid, Ø.; Børve, K. J. *J. Catal.* **2002**, *205*, 177.

(33) Costa, D.; Martra, G.; Che, M.; Manceron, L.; Kermanec, M. *J. Am. Chem. Soc.* **2002**, *124*, 7210.

(34) Smirnov, V. V.; Golubeva, E. N. *J. Mol. Catal. A* **2000**, *158*, 487.

(35) Griffe, B.; Sierraalta, A.; Ruette, F.; Brito, J. *J. Mol. Catal. A: Chem.* **2001**, *168*, 265.

(36) Griffe, B.; Sierraalta, A.; Ruette, F.; Brito, J. *J. Mol. Struct. (THEOCHEM)* **2003**, *625*, 59.

(37) Wheaton, V.; Majumdar, D.; Balasubramanian, K.; Chauffe, L.; Allen, P. G. *Chem. Phys. Lett.* **2003**, *371*, 349.

(38) Chang, C. M.; Jalnout, A. F.; Lin, C. *J. Mol. Struct. (THEOCHEM)* **2003**, *664*−*665*, 27.

(39) Bagatur'yants, A. A.; Ignatov, S. K.; Razuvaev, A. G.; Gropen, O. *Mater. Sci. Semicond. Process.* **2000**, *3*, 71.

(40) Puhakka, E.; Pakkanen, T. T.; Pakkanen, T. A. *Surf. Sci.* **1995**, *334*, 289.

(41) Hu, A.; Neyman, K. M.; Staufer, M.; Belling, T.; Gates, B. C.; Rösch, N. *J. Am. Chem. Soc.* **1999**, *121*, 4522.

(42) Neyman, K. M.; Vayssilov, G. N.; Rösch, N. *J. Organomet. Chem.* **2004**, *689*, 4384.

(43) Goellner, J. F.; Gates, B. C.; Vayssilov, G. N.; Rösch, N. *J. Am. Chem. Soc.* **2000**, *122*, 8056.

(44) Vayssilov, G. N.; Rösch, N. *J. Am. Chem. Soc.* **2002**, *124*, 3783.

(45) Suvanto, S.; Hirva, P.; Pakkanen, T. A. *Surf. Sci.* **2000**, *465*, 277.

(46) Duchateau, R.; Cremer, U.; Harmsen, R. J.; Mohamud, S. I.; Abbenhuis, H. C. L.; van Santen, R. A.; Meetsma, A.; Thiele, S. K. H.; van Tol, M. F. H.; Kranenburg, M. *Organometallics* **1999**, *18*, 5447.

(47) Belanzoni, P.; Rosi, M.; Sgamellotti, A. *J. Mol. Struct. (THEOCHEM)* **2002**, *579*, 181.

(48) Laurencin, D.; Villanneau, R.; Gérard, H.; Proust, A. *J. Phys. Chem. A* **2006**, *110*, 6345.

(49) Solans-Montfort, X.; Filhol, J.-S.; Coperet, C.; Eisenstein, O. *New J. Chem.* **2006**, *30*, 842.

(50) Rhers, B.; Salameh, A.; Baudoin, A.; Quadrelli, E. A.; Taoufik, M.; Copéret, C.; Lefebvre, F.; Basset, J. M.; Solans-Monfort, X.; Eisenstein, O.; Lukens, W. W.; Lopez, L. P. H.; Sinha, A.; Schrock, R. R. *Organometallics* **2006**, *25*, 3554.

(51) Motta, A.; Fragalà, I. L.; Marks, T. J. *J. Am. Chem. Soc.* **2008**, *130*, 16533.

(52) LeRoux, E.; Taoufik, M.; Copéret, C.; de Mallmann, A.; Thivolle-Cazat, J.; Basset, J. M.; Maunders, B. M.; Sunley, G. J. *Angew. Chem., Int. Ed.* **2005**, *44*, 6755.

(53) Taniike, T.; Tada, M.; Morikawa, Y.; Sasaki, T.; Iwasawa, Y. *J. Phys. Chem. B* **2006**, *110*, 4929.

(54) Mikhailov, M. N.; Bagatur'yants, A. A.; Kustov, L. M. *Russ. Chem. Bull., Int. Ed.* **2003**, *52*, 30.

(55) Mikhailov, M. N.; Bagatur'yants, A. A.; Kustov, L. M. *Russ. Chem. Bull., Int. Ed.* **2003**, *52*, 1928.

(56) Mikhailov, M. N.; Kustov, L. M. *Russ. Chem. Bull., Int. Ed.* **2005**, *54*, 300.

(57) Besedin, D. V.; Ustynyuk, L. Yu.; Ustynyuk, Y. A.; Lunin, V. V. *Top. Catal.* **2005**, *32*, 47.

(58) Thieuleux, C.; Quadrelli, E. A.; Basset, J.-M.; Döbler, J.; Sauer, J. *Chem. Commun.* **2004**, 1729.

(59) Copéret, C.; Grouillet, A.; Basset, J.-M.; Chermette, H. *ChemPhysChem* **2003**, *4*, 608.

(60) Mortensen, J. J.; Parrinello, M. *J. Phys. Chem. B* **2000**, *104*, 2901.

(61) Joubert, J.; Delbecq, F.; Thieuleux, C.; Taoufik, M.; Blanc, F.; Copéret, C.; Thivolle-Cazat, J.; Basset, J. M.; Sautet, P. *Organometallics* **2007**, *26*, 3329.

(62) Joubert, J.; Delbecq, F.; Copéret, C.; Basset, J. M.; Sautet, P. *Top. Catal.* **2008**, *48*, 114.

(63) Joubert, J.; Delbecq, F.; Sautet, P. *J. Catal.* **2007**, *251*, 507.

(64) Joubert, J.; Salameh, A.; Krakoviack, V.; Delbecq, F.; Sautet, P.; Copéret, C.; Basset, J.-M. *J. Phys. Chem. B* **2006**, *110*, 23944.

(65) Solans-Monfort, X.; Clot, E.; Copéret, C.; Eisenstein, O. *J. Am. Chem. Soc.* **2005**, *127*, 14015.

(66) Poater, A.; Solans-Monfort, X.; Clot, E.; Copéret, C.; Eisenstein, O. *J. Am. Chem. Soc.* **2007**, *129*, 8207.

(67) Leduc, A.-M.; Salameh, A.; Soulivong, D.; Chabanas, M.; Basset, J.-M.; Copéret, C.; Solans-Monfort, X.; Clot, E.; Eisenstein, O.; Böhm, V. P. W.; Röper, M. *J. Am. Chem. Soc.* **2008**, *130*, 6288.

(68) Handzlik, J.; Ogonowski, J. *J. Mol. Catal. A: Chem.* **2001**, *175*, 215.

(69) Handzlik, J.; Ogonowski, J. *J. Mol. Catal. A: Chem.* **2002**, *184*, 371.

(70) Handzlik, J. *J. Catal.* **2003**, *220*, 23.

(71) Handzlik, J. *Surf. Sci.* **2004**, *562*, 101.

(72) Handzlik, J.; Ogonowski, J.; Tokarz-Sobieraj, R. *Catal. Today* **2005**, *101*, 163.

(73) Handzlik, J. *J. Mol. Catal. A: Chem.* **2004**, *218*, 91.

(74) Handzlik, J. *Surf. Sci.* **2007**, *601*, 2054.

(75) Handzlik, J. *J. Phys. Chem. B* **2005**, *109*, 20794.

(76) Handzlik, J.; Sautet, P. *J. Catal.* **2008**, *256*, 1.

(77) Handzlik, J.; Sautet, P. *J. Phys. Chem. C* **2008**, *112*, 14456.

(78) Schinzel, S.; Chermette, H.; Copéret, C.; Basset, J. M. *J. Am. Chem. Soc.* **2008**, *130*, 7984.

(79) Espelid, Ø.; Børve, J. K. *J. Catal.* **2000**, *195*, 125.

(80) Espelid, Ø.; Børve, J. K. *J. Catal.* **2002**, *205*, 366.

(81) Espelid, Ø.; Børve, J. K. *J. Catal.* **2002**, *206*, 331.

(82) Boero, M.; Parrinello, M.; Terakura, K. *J. Am. Chem. Soc.* **1998**, *120*, 2746.

(83) Kawamura-Kuribayashi, H.; Koga, N.; Morokuma, K. *J. Am. Chem. Soc.* **1992**, *114*, 2359.

(84) Boero, M.; Parrinello, M.; Hüffer, S.; Weiss, H. *J. Am. Chem. Soc.* **2000**, *122*, 501.

(85) Boero, M.; Parrinello, M.; Weiss, H.; Hüffer, S. *J. Phys. Chem. A* **2001**, *105*, 5096.